



TECH BRIEFS

NATIONAL AERONAUTICS AND SPACE ADMINISTRATION

-  **Technology Focus**
-  **Electronics/Computers**
-  **Software**
-  **Materials**
-  **Mechanics**
-  **Machinery/Automation**
-  **Manufacturing & Prototyping**
-  **Bio-Medical**
-  **Physical Sciences**
-  **Information Sciences**
-  **Books and Reports**

INTRODUCTION

Tech Briefs are short announcements of innovations originating from research and development activities of the National Aeronautics and Space Administration. They emphasize information considered likely to be transferable across industrial, regional, or disciplinary lines and are issued to encourage commercial application.

Availability of NASA Tech Briefs and TSPs

Requests for individual Tech Briefs or for Technical Support Packages (TSPs) announced herein should be addressed to

National Technology Transfer Center

Telephone No. (800) 678-6882 or via World Wide Web at www2.nttc.edu/leads/

Please reference the control numbers appearing at the end of each Tech Brief. Information on NASA's Innovative Partnerships Program (IPP), its documents, and services is also available at the same facility or on the World Wide Web at <http://ipp.nasa.gov>.

Innovative Partnerships Offices are located at NASA field centers to provide technology-transfer access to industrial users. Inquiries can be made by contacting NASA field centers listed below.

NASA Field Centers and Program Offices

Ames Research Center

Lisa L. Lockyer
(650) 604-1754
lisa.l.lockyer@nasa.gov

Dryden Flight Research Center

Gregory Poteat
(661) 276-3872
greg.poteat@dfrc.nasa.gov

Goddard Space Flight Center

Nona Cheeks
(301) 286-5810
nona.k.cheeks@nasa.gov

Jet Propulsion Laboratory

Ken Wolfenbarger
(818) 354-3821
james.k.wolfenbarger@jpl.nasa.gov

Johnson Space Center

Michele Brekke
(281) 483-4614
michele.a.brekke@nasa.gov

Kennedy Space Center

Jim Aliberti
(321) 867-6224
Jim.Aliberti@nasa.gov

Langley Research Center

Martin Waszak
(757) 864-4052
martin.r.waszak@nasa.gov

Glenn Research Center

Robert Lawrence
(216) 433-2921
robert.f.lawrence@nasa.gov

Marshall Space Flight Center

Vernotto McMillan
(256) 544-2615
vernotto.mcmillan@msfc.nasa.gov

Stennis Space Center

John Bailey
(228) 688-1660
john.w.bailey@nasa.gov

Carl Ray, Program Executive

Small Business Innovation
Research (SBIR) & Small
Business Technology
Transfer (STTR) Programs
(202) 358-4652
carl.g.ray@nasa.gov

Merle McKenzie

Innovative Partnerships
Program Office
(202) 358-4652
merle.mckenzie-1@nasa.gov



TECH BRIEFS

NATIONAL AERONAUTICS AND SPACE ADMINISTRATION



5 Technology Focus: Data Acquisition

- 5 Measurement and Controls Data Acquisition System
- 5 IMU/GPS System Provides Position and Attitude Data
- 5 Using Artificial Intelligence to Inform Pilots of Weather
- 6 Fast Lossless Compression of Multispectral-Image Data
- 8 Developing Signal-Pattern-Recognition Programs
- 9 Implementing Access to Data Distributed on Many Processors



11 Electronics/Computers

- 11 Compact, Efficient Drive Circuit for a Piezoelectric Pump
- 12 Dual Common Planes for Time Multiplexing of Dual-Color QWIPs
- 13 MMIC Power Amplifier Puts Out 40 mW From 75 to 110 GHz



15 Software

- 15 2D/3D Visual Tracker for Rover Mast
- 15 Adding Hierarchical Objects to Relational Database General-Purpose XML-Based Information Managements



17 Materials

- 17 Vaporizable Scaffolds for Fabricating Thermoelectric Modules
- 18 Producing Quantum Dots by Spray Pyrolysis



19 Machinery/Automation

- 19 Mobile Robot for Exploring Cold Liquid/Solid Environments

- 20 System Would Acquire Core and Powder Samples of Rocks



21 Manufacturing & Prototyping

- 21 Improved Fabrication of Lithium Films Having Micron Features
- 22 Manufacture of Regularly Shaped Sol-Gel Pellets



23 Bio-Medical

- 23 Regulating Glucose and pH, and Monitoring Oxygen in a Bioreactor



25 Physical Sciences

- 25 Satellite Multiangle Spectropolarimetric Imaging of Aerosols
- 26 Interferometric System for Measuring Thickness of Sea Ice
- 27 Microscale Regenerative Heat Exchanger



29 Information Sciences

- 29 Protocols for Handling Messages Between Simulation Computers
- 30 Statistical Detection of Atypical Aircraft Flights
- 30 NASA's Aviation Safety and Modeling Project



33 Books & Reports

- 33 Multimode-Guided-Wave Ultrasonic Scanning of Materials
- 33 Algorithms for Maneuvering Spacecraft Around Small Bodies
- 33 Improved Solar-Radiation-Pressure Models for GPS Satellites
- 33 Measuring Attitude of a Large, Flexible, Orbiting Structure

This document was prepared under the sponsorship of the National Aeronautics and Space Administration. Neither the United States Government nor any person acting on behalf of the United States Government assumes any liability resulting from the use of the information contained in this document, or warrants that such use will be free from privately owned rights.



Technology Focus: Data Acquisition

Measurement and Controls Data Acquisition System

Marshall Space Flight Center, Alabama

Measurement and Controls Data Acquisition System (MCDAS) is an application program that integrates the functions of two stand-alone programs: one for acquisition of data, the other for controls. MCDAS facilitates and improves testing of complex engineering systems by helping to perform calibration and setup of test systems and acquisition, dissemination, and processing of data. Features of MCDAS include an intuitive, user-friendly graphical user interface, a capability for acquiring data at rates greater than previously possible,

cooperation between the data-acquisition software subsystem and alarm-checking and analytical components of the control software subsystem, and a capability for dissemination of data through fiber optics and virtual and wide-area networks, including networks that contain hand-held display units. The integration of the data acquisition and control software offers a safety advantage by making alarm information available to the control software in a more timely manner. By enabling the use of hand-held devices, MCDAS re-

duces the time spent by technicians asking for screen updates to determine effects of setup actions. Previously recorded data can be processed without interruption to current acquisition of data. Analysts can continue to view test parameters while test-data files are being generated.

This program was written by Rick Hall of Marshall Space Flight Center, Alice Daniel formerly of UNITes (NTSI), and Frank E. Batts, Sr. of Langley Research Center. Further information is contained in a TSP (see page 1). MFS-32014-1

IMU/GPS System Provides Position and Attitude Data

Stennis Space Center, Mississippi

A special navigation system is being developed to provide high-quality information on the position and attitude of a moving platform (an aircraft or spacecraft), for use in pointing and stabilization of a hyperspectral remote-sensing system carried aboard the platform. The system also serves to enable synchronization and interpretation of readouts of all onboard sensors. The heart of the system is a commercially available unit, small enough to be held in one hand, that contains an integral combination of an inertial measurement unit (IMU) of the microelectromechanical systems (MEMS) type, Global Positioning System (GPS)

receivers, a differential GPS subsystem, and ancillary data-processing subsystems. The system utilizes GPS carrier-phase measurements to generate time data plus highly accurate and continuous data on the position, attitude, rotation, and acceleration of the platform. Relative to prior navigation systems based on IMU and GPS subsystems, this system is smaller, is less expensive, and performs better. Optionally, the system can easily be connected to a laptop computer for demonstration and evaluation. In addition to airborne and spaceborne remote-sensing applications, there are numerous potential terrestrial sensing,

measurement, and navigation applications in diverse endeavors that include forestry, environmental monitoring, agriculture, mining, and robotics.

This work was done by Ching Fang Lin of American GNC Corp. for Stennis Space Center.

*Inquiries concerning rights for the commercial use of this invention should be addressed to: American GNC Corporation
888 Easy Street
Simi Valley, CA 93065
E-mail: cflin@americangnc.com
Refer to SSC-00225, volume and number of this NASA Tech Briefs issue, and the page number.*

Using Artificial Intelligence to Inform Pilots of Weather

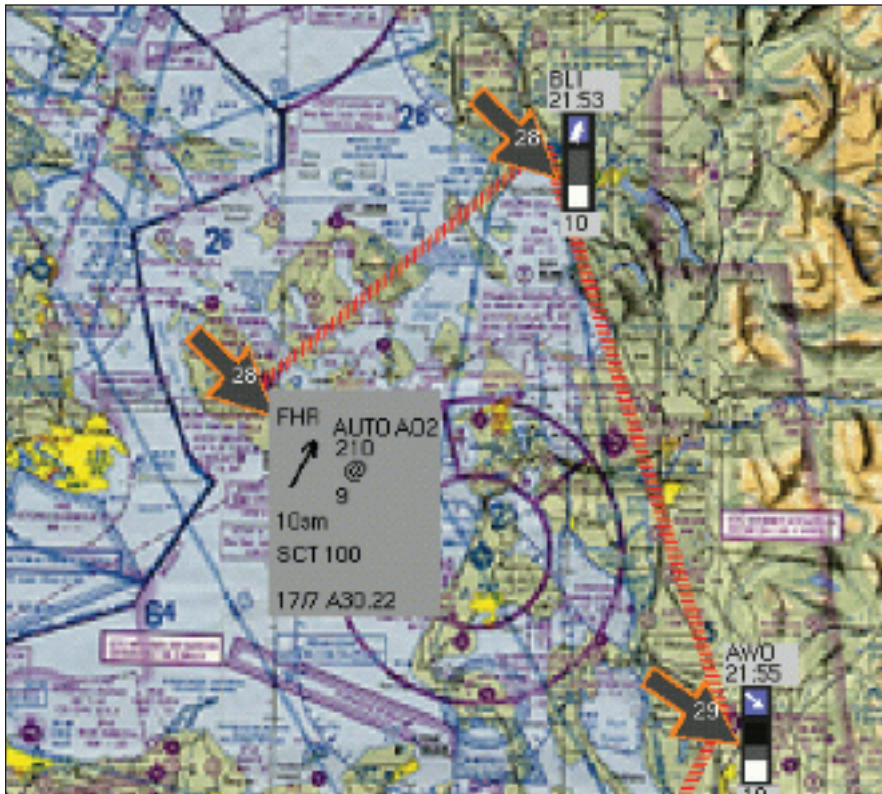
Weather awareness is increased; workload is reduced.

Ames Research Center, Moffett Field, California

An automated system to assist a General Aviation (GA) pilot in improving situational awareness of weather in flight is now undergoing development. This development is prompted by the observation that most fatal GA accidents are attributable to loss of weather awareness. Loss of weather awareness, in turn, has been attributed to the diffi-

culty of interpreting traditional pre-flight weather briefings and the difficulty of both obtaining and interpreting traditional in-flight weather briefings. The developmental automated system not only improves weather awareness but also substantially reduces the time a pilot must spend in acquiring and maintaining weather awareness.

The automated system includes computer hardware and software, a speech-based hardware/software user interface, and hardware interfaces between the computer and aircraft radio-communication equipment. The heart of the system consists of artificial-intelligence software, called Aviation Weather Environment (AWE), that implements a



Current Weather and Winds Aloft are shown alongside a pilot-selected route. Wind velocity at the pilot-selected altitude is depicted graphically with black arrows. The current weather is shown using symbolic and textual representations.

human-centered methodology oriented towards providing the weather information (1) that the pilot needs and/or wants, (2) at the appropriate time, and (3) in the appropriate format.

AWE can be characterized as a context-aware, domain-and-task knowledgeable, personalized, adaptive assistant.

AWE automatically monitors weather reports for the pilot's flight route and warns the pilot of any weather conditions outside the limits of acceptable weather conditions that the pilot has specified in advance. AWE provides textual and/or graphical representations of important weather elements overlaid

on a navigation map (see figure). The representations depict current and forecast conditions in an easy-to-interpret manner and are geographically positioned next to each applicable airport to enable the pilot to visualize conditions along the route. In addition to automatic warnings, the system enables the pilot to verbally request (via the speech-based user interface) weather and airport information.

AWE is context-aware in the following sense: From the location of the aircraft (as determined by a Global Positioning System receiver) and the route as specified by the pilot, AWE determines the phase of flight. In determining the timing of warnings and the manner in which warnings are issued, AWE takes account of the phase of flight, the pilot's definition of acceptable weather conditions, and the pilot's preferences for automatic notification. By noting the pilot's verbal requests for information during the various phases of flight, the system learns to provide the information, without explicit requests, at the corresponding times on subsequent flights under similar conditions.

This work was done by Lilly Spirkovska of Ames Research Center and Suresh K. Lodha of the University of California. Further information is contained in a TSP (see page 1).

Inquiries concerning rights for the commercial use of this invention should be addressed to the Patent Counsel, Ames Research Center, (650) 604-5104. Refer to ARC-14970-1.

Fast Lossless Compression of Multispectral-Image Data

A low-complexity adaptive-filtering algorithm is used.

NASA's Jet Propulsion Laboratory, Pasadena, California

An algorithm that effects fast lossless compression of multispectral-image data is based on low-complexity, proven adaptive-filtering algorithms. This algorithm is intended for use in compressing multispectral-image data aboard spacecraft for transmission to Earth stations. Variants of this algorithm could be useful for lossless compression of three-dimensional medical imagery and, perhaps, for compressing image data in general.

The main adaptive-filtering algorithm on which the present algorithm is based is the sign algorithm (also known as the

sign-error algorithm and as the binary reinforcement algorithm). The sign algorithm is related to the least-mean-square (LMS) algorithm. Both algorithms are briefly described in the following two paragraphs.

Consider a sequence of image data (or any other data) that one seeks to compress. The sequence is specified in terms of a sequentially increasing index (k) and the value (d_k) of the k th sample. An estimated value of the k th sample, \hat{d}_k , is calculated by the equation

$$\hat{d}_k = \mathbf{w}_k^T \mathbf{u}_k,$$

where \mathbf{w}_k is a filter-weight vector at

index k and \mathbf{u}_k is an input vector that can be defined in any of a number of different ways, depending on the specific application. Once the estimate \hat{d}_k has been calculated, the error between the estimate and the exact value is calculated as

$$e_k = \hat{d}_k - d_k.$$

When the LMS algorithm or sign algorithm is used as part of a predictive compression scheme, the sequence of e_k values is encoded in the compressed bitstream.

The error value is also used to update the filter weights in either of two ways, de-

pending on which algorithm is in use. In the LMS algorithm, the update equation is

$$\mathbf{w}_{k+1} = \mathbf{w}_k - \mu \mathbf{u}_k e_k.$$

In the sign algorithm, the update equation is

$$\mathbf{w}_{k+1} = \mathbf{w}_k - \mu \mathbf{u}_k \text{sgn}(e_k).$$

In both update equations, μ is a positive, scalar step-size parameter that controls the trade-off between convergence speed and average steady-state error. A smaller value of μ results in better steady-state performance but slower convergence. In some variants of these algorithms, the value of μ changes over time.

In the present algorithm, the index k is taken as an abstract representation of three indices (x,y,z) that are the coordinates of the sample in the multispectral dataset. Specifically, x and y are the spatial coordinates and z denotes the spectral band. The signal level (equivalently, the sample value) for that location is represented by $d_k \equiv s(x,y,z)$.

For purposes of compression, an image represented by a stream of data to be compressed is partitioned spatially into conve-

niently sized, fixed regions. The data are compressed in the order in which they are received, maintaining separate statistics for each band and switching among the bands as necessary. The data from each region are compressed independently of those from other regions. Performing independent compression calculations for each region limits the adverse effect of loss of data.

The input vector \mathbf{u}_k chosen for this algorithm contains values from a six-sample prediction neighborhood of a sample of interest: three values from adjacent samples in the same spectral band and one sample each from the same location in each of three preceding spectral bands. Specifically,

$$\mathbf{u}_k = \begin{bmatrix} s(x-1,y,z) - \tilde{s}(x,y,z) \\ s(x-1,y-1,z) - \tilde{s}(x,y,z) \\ s(x,y-1,z) - \tilde{s}(x,y,z) \\ s(x,y,z-1) - \tilde{s}(x,y,z-1) \\ s(x,y,z-2) - \tilde{s}(x,y,z-2) \\ s(x,y,z-3) - \tilde{s}(x,y,z-3) \end{bmatrix}$$

where $\tilde{s}(x,y,z)$ is a mean value of previous samples in the vicinity of x,y in spectral band z . The stream of e_k values calculated by use of this \mathbf{u}_k is further compressed by use of Golomb codes.

In tests, the compression effectiveness of this algorithm was shown to be competitive with that of the best previously reported data-compression algorithms of similar complexity. The table presents results from one series of tests performed on multispectral imagery acquired by NASA's airborne visible/infrared imaging spectrometer (AVIRIS).

This work was done by Matthew Klimesh of Caltech for NASA's Jet Propulsion Laboratory. Further information is contained in a TSP (see page 1).

The software used in this innovation is available for commercial licensing. Please contact Karina Edmonds of the California Institute of Technology at (626) 395-2322. Refer to NPO-42517.

Scene	Present Algorithm		Other Algorithms				
	Fast Lossless	ICER-3D	JPEG-LS (2-D)	Rice/USES Multispectral	Differential JPEG-LS	SLSQ (Rizzo et al.)*	SLSQ-OPT (Rizzo et al.)*
Cuprite 1	4.89	5.14	7.13	6.00	5.44	5.03	4.90
Cuprite 2	5.02	5.34	7.50	6.13	5.58	5.09	4.97
Cuprite 3	4.92	5.16	7.16	6.00	5.45	5.06	4.92
Cuprite 4	4.98	5.21	7.16	6.05	5.51	5.10	4.96
Jasper Ridge 1	5.04	5.41	7.72	6.17	5.62	5.06	4.95
Jasper Ridge 2	5.02	5.37	7.67	6.12	5.59	5.05	4.94
Jasper Ridge 3	5.07	5.47	7.90	6.19	5.67	5.10	4.99
Jasper Ridge 4	5.07	5.47	7.87	6.22	5.67	5.11	5.00
Jasper Ridge 5	5.02	5.39	7.75	6.14	5.60	5.06	4.94
Low Altitude 1	5.37	5.70	7.81	6.53	5.97	5.38	5.30
Low Altitude 2	5.42	5.76	7.95	6.58	6.02	5.40	5.33
Low Altitude 3	5.30	5.58	7.57	6.42	5.88	5.33	5.23
Low Altitude 4	5.32	5.58	7.53	6.42	5.89	5.37	5.26
Low Altitude 4	5.37	5.63	7.60	6.47	5.91	5.40	5.30
Low Altitude 6	5.29	5.56	7.52	6.42	5.85	5.34	5.24
Low Altitude 7	5.29	5.60	7.64	6.43	5.88	5.34	5.24
Lunar Lake 1	4.99	5.19	6.98	6.02	5.49	5.12	4.99
Lunar Lake 2	4.94	5.14	6.96	5.97	5.44	5.07	4.93
Moffett Field 1	5.12	5.48	7.78	6.24	5.70	5.15	5.03
Moffett Field 2	5.11	5.40	7.57	6.20	5.60	5.08	4.98
Moffett Field 3	4.98	5.12	7.03	5.96	5.41	4.96	4.86
Average	5.12	5.41	7.51	6.22	5.68	5.17	5.06

* F. Rizzo, B. Carpentieri, G. Motta, and J.A. Storer, "Low-complexity lossless compression of hyperspectral imagery via linear prediction," *IEEE Signal Processing Letters*, 12(2):138-141, February 2005.

Data From AVIRIS Images of various scenes were compressed by the present algorithm and by a number of other algorithms. The numerical entries are the numbers of bits per sample in the compressed data streams.

➤ Developing Signal-Pattern-Recognition Programs

Software system aids development of application programs that analyze signals.

Lyndon B. Johnson Space Center, Houston, Texas

Pattern Interpretation and Recognition Application Toolkit Environment (PIRATE) is a block-oriented software system that aids the development of application programs that analyze signals in real time in order to recognize signal patterns that are indicative of conditions or events of interest. PIRATE was originally intended for use in writing application programs to recognize patterns in space-shuttle telemetry signals received at Johnson Space Center's Mission Control Center: application programs were sought to (1) monitor electric currents on shuttle ac power busses to recognize activations of specific power-consuming devices, (2) monitor various pressures and infer the states of affected systems by applying a Kalman filter to the pressure signals, (3) determine fuel-leak rates from sensor data, (4) detect faults in gyroscopes through analysis of system measurements in the frequency domain, and (5) determine drift rates in inertial measurement units by regressing measurements against time. PIRATE can also be used to develop signal-pattern-recognition software for different purposes — for example, to monitor and control manufacturing processes.

PIRATE was preceded by a custom stripchart-analysis program that took a long time to develop and offered little opportunity for reuse. Also available prior to the development of PIRATE were commercial block-oriented development software systems that were useful for prototyping but exhibited significant limitations: for example, they could not be used to produce real-time application programs, could not be used to develop software compatible with the hardware and the other software of the Mission Control Center, could not be used to develop application programs that could function in the face of the communication difficulties (especially, intermittency and errors) inherent in monitoring remote equipment, and could not provide pattern-recognition capabilities. PIRATE overcomes these deficiencies to a large extent, and goes beyond that by including a C-language interface that provides unprecedented flexibility.

PIRATE includes the following components:

- *The PIRATE data-flow language.* An application program is specified by use of the PIRATE data-flow language. An

application-program specification defines which data processing modules will be used in the program and establishes the data flowing among the modules. Similarly, for building a module, one specifies the flow of data into and out of a module by use of the PIRATE language.

- *The PIRATE predefined modules.* PIRATE contains several predefined modules, including ones for data communication, signal processing, and data filtering. Among these are software tools to filter out the highly non-Gaussian errors that are typical of the communication process while leaving the nonerroneous data intact. (Most other signal-processing software filters that can remove non-Gaussian errors also undesirably modify the underlying signals.) Also among the predefined modules are a Bayesian classifier and other software tools for interpreting the contents of signals.

- *The PIRATE code generator.* The PIRATE code generator translates an application-program-specification file and the associated module-configuration files into a standard C-language file. This file contains the main routine for the application program. A C compiler can then compile and link this file to produce an efficient real-time pattern-recognition application program.

- *The PIRATE object library.* The generated code makes calls to several PIRATE infrastructure routines. The PIRATE object library contains the object code for these infrastructure routines and for the predefined module routines.

- *The PIRATE "imake" facility.* The imake is a programming software tool that was developed to address issues of portability pertaining to the X Window System and to provide a high-level view of the software-building process. However, the standard imake suite explicitly targets the construction of X Window System software. The PIRATE imake facility takes advantage of the standard imake suite where practical, but targets the construction of PIRATE and PIRATE application programs rather than X Window System software.

- *An architecture for the development of modules by the user.* PIRATE is intentionally an open-ended software tool. While

simple application programs can be constructed by use of the predefined modules, it is likely that a useful pattern-recognition application programs could not. Instead, domain-specific logic can be expected to be necessary. PIRATE enables the implementation of domain-specific knowledge in the widely used C programming language. The architecture for user-developed modules specifies how such domain knowledge can be used in a PIRATE application program.

PIRATE is used both in building a pattern-recognition application program and in the real-time execution of that program. To build an application program, one constructs an application-specification file, application-specific modules, and application imake file. The imake file identifies the components that form the executable application program and directs construction of these components from the source files developed by the user.

During execution of the pattern-recognition application program, the source module of the program acquires the incoming data and uses the PIRATE infrastructure to feed the data to downstream modules. The infrastructure sends the appropriate data to the appropriate modules, which operate on the data. Each module uses the PIRATE infrastructure to send its output to modules downstream of it.

In PIRATE, transmission of data between data-processing modules is always performed by calls to C functions that are parts of an executable module. In other software systems, data are often transmitted between modules via operating systems; the computational overhead of doing so is often several orders of magnitude greater than that of PIRATE. In PIRATE, the processing of data within a module is performed by compiled functions. In other systems, the processing of data may be performed by interpreters, which, again entail computational overhead much greater than that of PIRATE.

This program was written by Robert O. Shelton of Johnson Space Center and David Hammen of LinCom. For further information, contact the Johnson Technology Transfer Office at (281) 483-3809. MSC-22944

● Implementing Access to Data Distributed on Many Processors

NASA's Jet Propulsion Laboratory, Pasadena, California

A reference architecture is defined for an object-oriented implementation of domains, arrays, and distributions written in the programming language Chapel. This technology primarily addresses domains that contain arrays that have regular index sets with the low-level implementation details being beyond the scope of this discussion. The theoretical foundations are based upon the work "A Semantic Framework for Domains, Arrays, and Distributions in Chapel" by Hans Zima. What is defined is a complete set of object-oriented operators that allows one to perform data distributions for domain arrays involving regular arithmetic index sets. What is unique is that these operators allow for the arbitrary regions of the arrays to be fragmented and distributed across multiple processors with a single point of access giving the programmer the illusion that all the elements are collocated on a single processor. Today's

massively parallel High Productivity Computing Systems (HPCS) are characterized by a modular structure, with a large number of processing and memory units connected by a high-speed network. Locality of access as well as load balancing are primary concerns in these systems that are typically used for high-performance scientific computation. Data distributions address these issues by providing a range of methods for spreading large data sets across the components of a system. Over the past two decades, many languages, systems, tools, and libraries have been developed for the support of distributions. Since the performance of data parallel applications is directly influenced by the distribution strategy, users often resort to low-level programming models that allow fine-tuning of the distribution aspects affecting performance, but, at the same time, are tedious and error-prone. This technology presents a reusable de-

sign of a data-distribution framework for data parallel high-performance applications. Distributions are a means to express locality in systems composed of large numbers of processor and memory components connected by a network. Since distributions have a great effect on the performance of applications, it is important that the distribution strategy is flexible, so its behavior can change depending on the needs of the application. At the same time, high productivity concerns require that the user be shielded from error-prone, tedious details such as communication and synchronization.

This program was written by Mark James of Caltech for NASA's Jet Propulsion Laboratory. Further information is contained in a TSP (see page 1).

This software is available for commercial licensing. Please contact Karina Edmonds of the California Institute of Technology at (626) 395-2322. Refer to NPO-42506.



Compact, Efficient Drive Circuit for a Piezoelectric Pump

Piezoelectric actuators are charged in a time much shorter than the pump cycle.

Lyndon B. Johnson Space Center, Houston, Texas

Figure 1 depicts a switching circuit that drives a piezoelectric pump at a high voltage with a polarity that alternates at the desired mechanical pump frequency. This circuit offers advantages of (1) high energy efficiency relative to conventional direct-drive circuits and (2) compactness relative to conventional resonant drive circuits.

Conventional direct-drive circuits are inefficient because the piezoelectric actuators in the pump behave electrically as large capacitors and consume only a small part of the energy supplied to them during each pump cycle. Conventional resonant drive circuits are more efficient, but they must include inductive coils, which can be unacceptably large.

The present switching drive circuit includes inductive coils, but they are small and not used to resonate the actuator capacitance; instead, the charging of the

actuator capacitances and the exchanges of energy among inductive and capacitive circuit elements are accomplished (by design) in times much shorter than the mechanical pump cycle. In other words, this drive circuit rapidly charges the actuator capacitance and turns itself off until the actuators reach their maximum mechanical expansion or contraction. Some time after the actuators reach their maximum mechanical expansion or contraction, the circuit turns itself back on to charge the actuator capacitance in the opposite polarity; as it does so, it replenishes the energy lost since the previous charge.

When power is first turned on, the capacitance of the piezoelectric actuators (C2 in Figure 1) is first charged to a potential of +450 V via transistor Q2. The charging current and, hence, charging time are determined by the characteristics of the

dc-to-dc converter and the characteristics of the piezoelectric films. Inductor L1 is used to reduce the initial current spike during each recharge cycle, and C1 is used to stabilize the output voltage of the converter as well as reduce the peak output current demand on the dc-to-dc converter. Inductor L2 is the main energy-storage inductor; it is used to exchange energy with C2 for switching polarity, as described in more detail below.

The timing signals that govern the operation of this circuit are transistor/transistor-logic (TTL)-level pulses with a duration of 5 ms and a repetition frequency equal to the desired pump frequency (20 Hz in the original design). The short pulse duration is necessary in order to enable the triac (Q2) to turn itself off when the current in inductor L2 reaches zero. The timing signal is generated by timing/control oscillator U6, which supplies

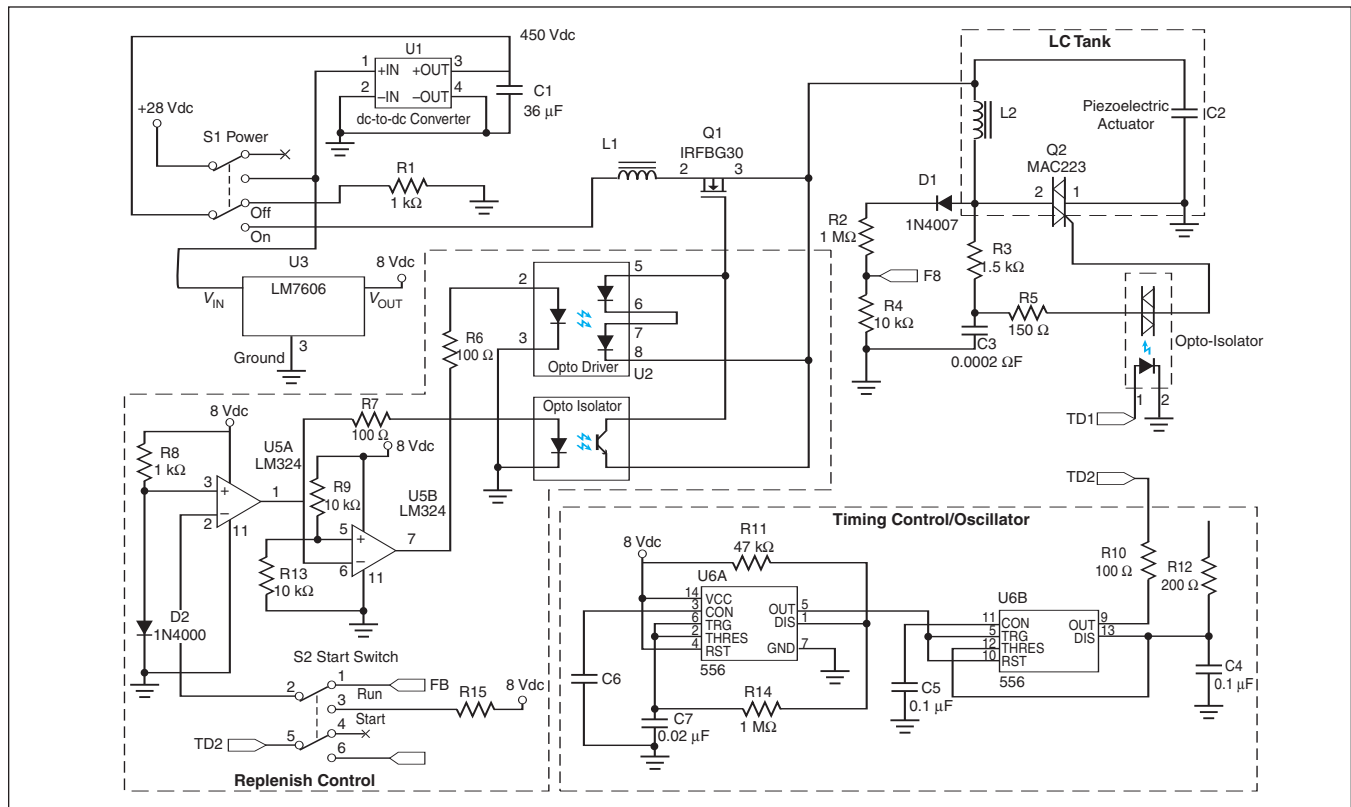


Figure 1. This Circuit Operates at High Efficiency in driving a piezoelectric pump at a frequency of 20 Hz. High efficiency is achieved by use of nonresonant inductor L2 to recycle the charge on the piezoelectric-actuator capacitance C2.

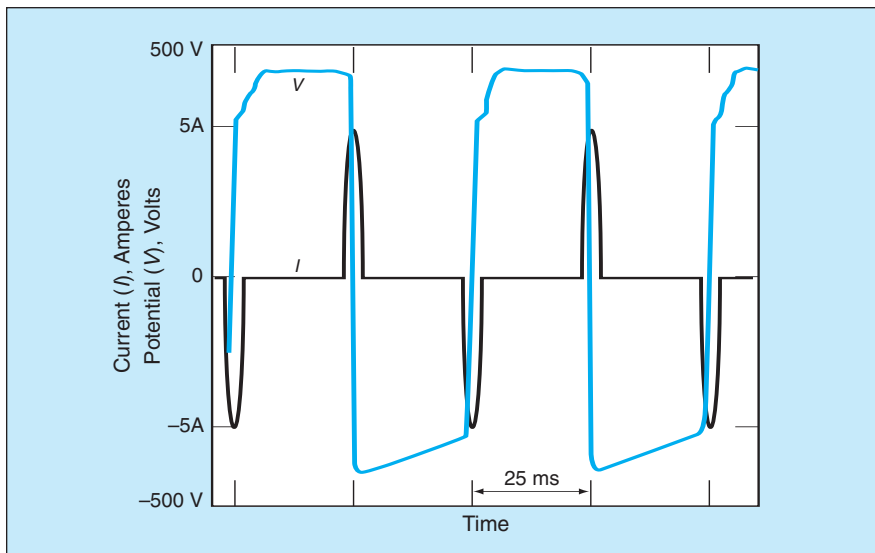


Figure 2. These Voltage and Current Waveforms occur at the terminals of the piezoelectric actuators.

timing drive current to opto-isolator U4, which, in turn, provides the switch-on signal for the triac gate.

Figure 2 illustrates the voltage and current waveforms at the terminals of the piezoelectric actuators. Suppose that C2 has been initially charged. At the beginning of the first half cycle, when a timing pulse occurs, the triac is turned on and current begins to flow from C2 through the triac and L2. When the magnitude of the current increases above the minimum hold current, the triac becomes latched on. The triac then continues to conduct until the current drops below the minimum hold current, which is essentially zero for the purpose of this application. The minimum hold current is reached and the triac turns off when the voltage on C2 reaches a negative peak near -450

V. The reversal of polarity is provided by L2. The precise magnitude of the peak reverse voltage is slightly less than |450 V| by an amount that depends on the energy lost in the various exchanges of energy involved in the reversal of polarity. While the triac remains off, C2 remains in its negatively charged state, in which only parasitic dielectric losses slowly reduce the magnitude of the voltage on C2.

At the beginning of the second half cycle, when the next timing pulse arrives, the process described in the preceding paragraph is repeated, except that the currents and voltages applied to C2 are reversed. Again, the difference between |450 V| and the magnitude of the peak voltage depends on the energy lost.

If the operation as described thus far were allowed to continue, the voltages

would continue to decay and operation would halt after a number of cycles. To enable continuous operation, it is necessary to replenish the energy lost. This is accomplished as follows: After the completion of the polarity reversal of the second half cycle and before the arrival of the next timing pulse, the replenish-control subcircuit senses the triac cutoff and turns on Q1 to recharge C2 to 450 V. At the chosen 20-Hz pump frequency, the triac-off time is long enough to enable C2 to be recharged to 450 V by use of relatively low charging current, provided that the energy lost is relatively low.

Because recharging is done only during the positive half cycle, a dc offset is induced in C2; however, this offset is typically a small fraction of the peak drive voltage and does not adversely affect the operation of the piezoelectric actuators. The advantage of recharging only during positive half cycle is that the circuit can be less complex and contain fewer components than would be needed for recharging during both half cycles.

This work was done by Chris Matice of Stress Engineering Services Inc., and Frank E. Sager and Bill Robertson of Oceaneering Space Systems for Johnson Space Center.

Title to this invention has been waived under the provisions of the National Aeronautics and Space Act (42 U.S.C. 2457(f)) to Oceaneering Space Systems. Inquiries concerning licenses for its commercial development should be addressed to:

*Oceaneering Space Systems
16665 Space Center Blvd.*

Houston, TX 77058-2268

Refer to MSC-22887, volume and number of this NASA Tech Briefs issue, and the page number.

Dual Common Planes for Time Multiplexing of Dual-Color QWIPs

With external control, commercial single-color readout integrated circuits could be used.

NASA's Jet Propulsion Laboratory, Pasadena, California

A proposed improved method of externally controlled time multiplexing of the readouts of focal-plane arrays of pairs of stacked quantum-well infrared photodetectors (QWIPs) that operate in different wavelength bands is based on a dual-detector-common-plane circuit configuration. The method would be implemented in a QWIP integrated-circuit chip hybridized with a readout integrated-circuit (ROIC) chip.

There are alternative methods of multicolor readout, but they involve more on-chip circuitry and the attendant disadvantages of greater size, power dissipation, number of control signals, and complexity of circuitry on the QWIP and ROIC chips. To minimize size of, and power dissipation in, a multicolor pixel, one must minimize the number of transistors and control signals; this can be achieved only by time multiplexing of

colors in each pixel. The time multiplexing can be controlled by signals from external or internal circuitry. The proposed reliance on external control for time multiplexing would make it possible to use a commercial single-color ROIC with only minor modifications in the form of extra metallization for an additional detector common plane and for clocking bias potentials. (If, instead, one were to rely on internally controlled

multiplexing, it would be necessary to radically redesign the ROIC, at considerably greater development cost.) Other advantages of the external-control approach are greater flexibility and the possibility of using a technique, known as “skimming,” for subtracting unwanted dark-, background-, and noise-current contributions from readout signals

The figure schematically depicts the circuitry in one pixel according to an internally controlled multiplexing scheme and according to the proposed externally controlled multiplexing scheme. In both schemes, the time multiplexing would be accomplished by switching

(clocking or ramping) the biases applied to the QWIPs via detector common planes. In the internal-control case, a bias signal would be applied via a single detector common plane and two internal electronic switches. In the proposed external-control case, bias signals would be applied via two detector common planes, without internal electronic switches. A previously unmentioned advantage of the external-control scheme shown in the figure is the need for only one indium bump (instead of two) in each pixel.

This work was done by Sir B. Rafol, Sarath Gunapala, Sumith Bandara, John Liu, and Jason Mumolo of Caltech for NASA's Jet

Propulsion Laboratory. Further information is contained in a TSP (see page 1).

In accordance with Public Law 96-517, the contractor has elected to retain title to this invention. Inquiries concerning rights for its commercial use should be addressed to:

*Innovative Technology Assets Management
JPL*

*Mail Stop 202-233
4800 Oak Grove Drive
Pasadena, CA 91109-8099
(818) 354-2240*

*E-mail: iaoffice@jpl.nasa.gov
Refer to NPO-30523, volume and number of this NASA Tech Briefs issue, and the page number.*

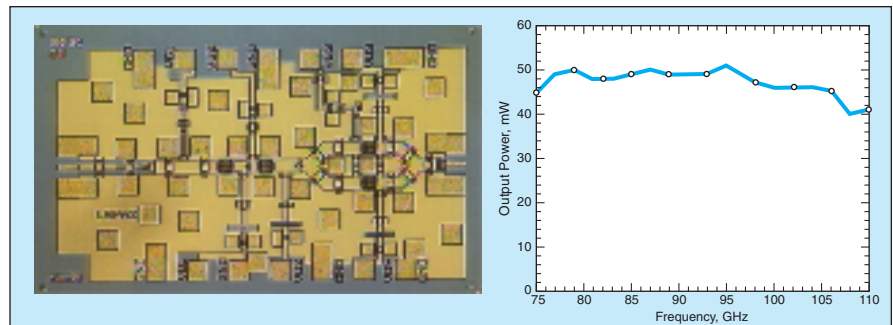
MMIC Power Amplifier Puts Out 40 mW From 75 to 110 GHz

This amplifier operates over the full frequency band of the WR-10 waveguide.

NASA's Jet Propulsion Laboratory, Pasadena, California

A three-stage monolithic microwave integrated circuit (MMIC) W-band amplifier has been constructed and tested in a continuing effort to develop amplifiers as well as oscillators, frequency multipliers, and mixers capable of operating over wide frequency bands that extend above 100 GHz. There are numerous potential uses for MMICs like these in scientific instruments, radar systems, communication systems, and test equipment operating in this frequency range.

This amplifier can be characterized, in part, as a lower-frequency, narrower-band, higher-gain version of the one described in “Power Amplifier With 9 to 13 dB of Gain from 65 to 146 GHz” (NPO-20880), *NASA Tech Briefs*, Vol. 25, No. 1 (January 2001), page 44. This amplifier includes four InP high-electron-mobility transistors (HEMTs), each having a gate periphery of 148 μm . In the third amplifier stage, two of the HEMTs are combined in parallel to maximize the output power. The amplifier draws



The Amplifier Shown in the Photograph was tested at a supply potential of 2.5 V, a gate bias potential of -0.05 V, and an input excitation power of 2 mW at frequencies from 75 to 110 GHz. The plot of output power vs. frequency can be characterized by a large-signal gain of about 13.5 ± 0.5 dB. (Note: The amplifier is actually about 2 mm long.)

a current of 250 mA at a supply potential of 2.5 V.

In a test, this amplifier was driven by a backward-wave oscillator set to provide an input power of 2 mW. The output power of the amplifier was measured by a power meter equipped with a WR-10 waveguide sensor. As shown in the figure, the amplifier put out a power between 40 and 50 mW over the frequency

range of 75 to 110 GHz, which is the entire frequency band of the WR-10 waveguide. At the stated power levels, this amplifier offers a power-added efficiency of slightly more than 6 percent.

This work was done by Lorene Samoska of Caltech for NASA's Jet Propulsion Laboratory. Further information is contained in a TSP (see page 1). NPO-30577



2D/3D Visual Tracker for Rover Mast

A visual-tracker computer program controls an articulated mast on a Mars rover to keep a designated feature (a target) in view while the rover drives toward the target, avoiding obstacles. Several prior visual-tracker programs have been tested on rover platforms; most require very small and well-estimated motion between consecutive image frames — a requirement that is not realistic for a rover on rough terrain. The present visual-tracker program is designed to handle large image motions that lead to significant changes in feature geometry and photometry between frames. When a point is selected in one of the images acquired from stereoscopic cameras on the mast, a stereo triangulation algorithm computes a three-dimensional (3D) location for the target. As the rover moves, its body-mounted cameras feed images to a visual-odometry algorithm, which tracks two-dimensional (2D) corner features and computes their old and new 3D locations. The algorithm rejects points, the 3D motions of which are inconsistent with a rigid-world constraint, and then computes the apparent change in the rover pose (i.e., translation and rotation). The mast pan and tilt angles needed to keep the target centered in the field-of-view of the cameras (thereby minimizing the area over which the 2D-tracking algorithm must operate) are computed from the estimated change in the rover pose, the 3D position of the target feature, and a model of kinematics of the

mast. If the motion between the consecutive frames is still large (i.e., 3D tracking was unsuccessful), an adaptive view-based matching technique is applied to the new image. This technique uses correlation-based template matching, in which a feature template is scaled by the ratio between the depth in the original template and the depth of pixels in the new image. This is repeated over the entire search window and the best correlation results indicate the appropriate match. The program could be a core for building application programs for systems that require coordination of vision and robotic motion.

This program was written by Max Bajracharya, Richard W. Madison, and Issa A. Nesnas of Caltech for NASA's Jet Propulsion Laboratory, and Esfandiar Bandari, Clayton Kunz, Matt Deans, and Maria Bualat of Ames Research Center. Further information is contained in a TSP (see page 1).

This software is available for commercial licensing. Please contact Karina Edmonds of the California Institute of Technology at (626) 395-2322. Refer to NPO-40696.

Adding Hierarchical Objects to Relational Database General-Purpose XML-Based Information Managements

NETMARK is a flexible, high-throughput software system for managing, storing, and rapid searching of unstructured and semi-structured documents. NETMARK transforms such documents from their original highly complex, constantly changing, heterogeneous data formats into well-

structured, common data formats in using Hypertext Markup Language (HTML) and/or Extensible Markup Language (XML). The software implements an object-relational database system that combines the best practices of the relational model utilizing Structured Query Language (SQL) with those of the object-oriented, semantic database model for creating complex data. In particular, NETMARK takes advantage of the Oracle 8i object-relational database model using physical-address data types for very efficient keyword searches of records across both context and content. NETMARK also supports multiple international standards such as WEBDAV for drag-and-drop file management and SOAP for integrated information management using Web services. The document-organization and -searching capabilities afforded by NETMARK are likely to make this software attractive for use in disciplines as diverse as science, auditing, and law enforcement.

This program was written by Shu-Chun Lin and Chris Knight of Ames Research Center; Tracy La of Computer Science Corporation; David Maluf and David Bell of Universities Space Research; Khai Peter Tran of QSS Group, Inc.; and Yuri Gawdiak of NASA Headquarters. Further information is contained in a TSP (see page 1).

This invention has been patented by NASA (U.S. Patent No. 6,968,338). Inquiries concerning rights for the commercial use of this invention should be addressed to the Ames Technology Partnerships Division at (650) 604-2954. Refer to ARC-14662-1.



Vaporizable Scaffolds for Fabricating Thermoelectric Modules

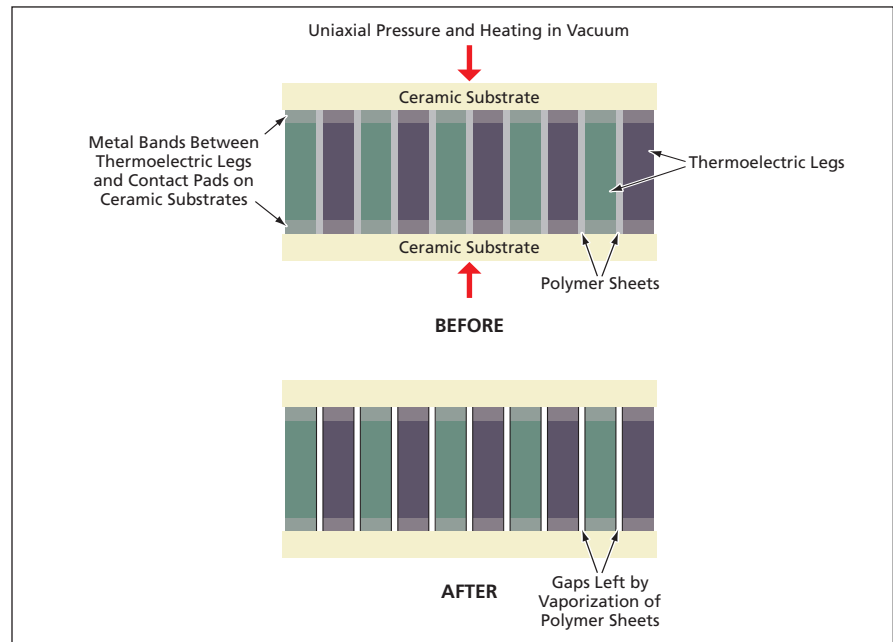
Thermoelectric legs would be separated by precise gaps.

NASA's Jet Propulsion Laboratory, Pasadena, California

A process for fabricating thermoelectric modules with vacuum gaps separating the thermoelectric legs has been conceived, and the feasibility of some essential parts of the process has been demonstrated. The vacuum gaps are needed to electrically insulate the legs from each other. The process involves the use of scaffolding in the form of sheets of a polymer to temporarily separate the legs by the desired distance, which is typically about 0.5 mm. During a bonding subprocess that would take place in a partial vacuum at an elevated temperature, the polymer would be vaporized, thereby creating the vacuum gaps. If desired, the gaps could later be filled with an aerogel for thermal insulation and to suppress sublimation of thermoelectric material, as described in "Aerogels for Thermal Insulation of Thermoelectric Devices" (NPO-40630), *NASA Tech Briefs*, Vol. 30, No. 7 (July, 2006), page 50.

A simple thermoelectric module would typically include thermoelectric legs stacked perpendicularly between metal contact pads on two ceramic substrates (see figure). As the design of the thermoelectric module and the fabrication process are now envisioned, the metal contact pads on the ceramic substrates would be coated with a suitable bonding metal (most likely, titanium), and the thermoelectric legs would be terminated in a possibly different bonding metal (most likely, molybdenum). Prior to stacking of the thermoelectric pads between the metal pads on the ceramic substrates, the polymer sheets would be bonded to the appropriate sides of the thermoelectric legs. After stacking, the resulting sandwich structure would be subjected to uniaxial pressure during heating in a partial vacuum to a temperature greater than 700 °C. The heating would bond the metal pads on the legs to the metal pads on the substrates and would vaporize the polymer sheets. The uniaxial pressure would hold the legs in place until bonding and vaporization were complete.

Ideally, the polymer chosen for use in this process should be sufficiently rigid



A Single Thermoelectric Module containing a small number of legs is shown here for simplicity to facilitate understanding of the process described in the text. In an economically practical version of the process, multiple modules would be stacked in a more-complex, checkerboardlike arrangement during bonding and vaporization of the polymer sheets.

to enforce dimensional stability of the gaps and should vaporize at a temperature low enough that it does not undergo pyrolysis. (Pyrolysis would create an undesired electrically conductive carbonaceous residue.) Poly(α -methylstyrene) [PAMS] has been selected as a promising candidate. PAMS is considered to be rigid, and, in a partial vacuum of 10^{-6} torr ($\approx 1.3 \times 10^{-4}$ Pa), it vaporizes in the temperature range of 250 to 400 °C, without pyrolyzing.

Initially, the primary concern raised by vaporization of polymer scaffolding was that polymer-vapor residue might interfere with the bonding of the thermoelectric legs to the metal pads on the ceramic substrates. In an experiment to investigate the likelihood of such interference, a mockup comprising two molybdenum legs separated by a PAMS sheet in contact with a titanium plate was placed under uniaxial pressure and heated to a temperature of 950 °C in a partial vacuum of 10^{-6} torr. Strong, uni-

form bonds were made between the molybdenum legs and the titanium plate, demonstrating that the PAMS vapor did not interfere with bonding.

This work was done by Jeffrey Sakamoto, Shiao-pin Yen, Jean-Pierre Fleurial, and Jong-Ah Paik of Caltech for NASA's Jet Propulsion Laboratory. Further information is contained in a TSP (see page 1).

In accordance with Public Law 96-517, the contractor has elected to retain title to this invention. Inquiries concerning rights for its commercial use should be addressed to:

*Innovative Technology Assets Management
JPL*

*Mail Stop 202-233
4800 Oak Grove Drive
Pasadena, CA 91109-8099
(818) 354-2240*

*E-mail: iaoffice@jpl.nasa.gov
Refer to NPO-41248 volume and number of this NASA Tech Briefs issue, and the page number.*

Producing Quantum Dots by Spray Pyrolysis

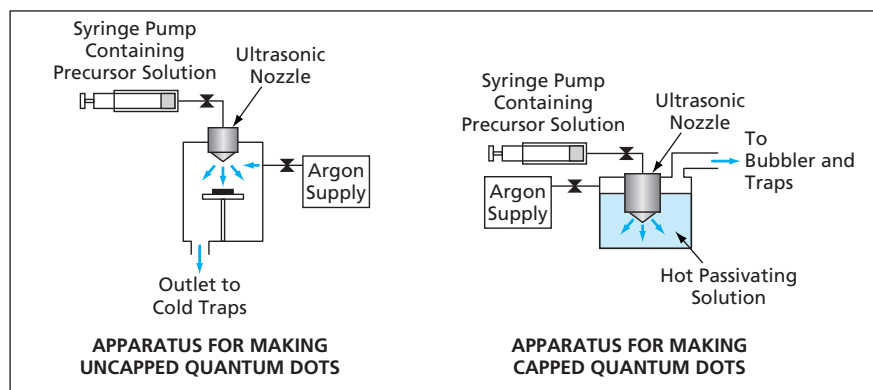
Sizes of quantum dots are determined by sizes of sprayed drops.

John H. Glenn Research Center, Cleveland, Ohio

An improved process for making nanocrystallites, commonly denoted quantum dots (QDs), is based on spray pyrolysis. Unlike the process used heretofore, the improved process is amenable to mass production of either passivated or non-passivated QDs, with computer control to ensure near uniformity of size.

The extraordinary optical properties that make QDs useful can be tailored via the chemical compositions and sizes of the QDs. Heretofore, QDs have been made by *in situ* pyrolysis of molecular reagents that contain all the elemental ingredients. In order to make all QDs in a batch have the same or nearly the same size, it is necessary to prevent nucleation with adjacent QDs by passivating the surfaces of the QDs soon after they have formed. Passivation is effected by use of a passivating coordinating solvent/ligand compound as one of the ingredients. This compound both serves as a medium for the formation of the QDs via pyrolysis and readily coordinates to the surfaces of the QDs, thereby preventing further nucleation. Covering of the surfaces of the QDs with the coordinating molecular groups is known in the art as capping. The capping groups can be organic or inorganic. The solvent/ligand can be formulated to tailor the surface properties of the QDs for a specific application. For example, they can be made hydrophilic or hydrophobic. Unfortunately, this *in situ* pyrolysis process cannot readily be scaled up to mass production, and the QDs produced exhibit excessive nonuniformity.

The improved process also includes py-



These Two Apparatuses serve to illustrate the basic principles of two variants of the spray-pyrolysis process for making uncapped or capped QDs of controlled size.

rolysis, but differs from the prior process in the pyrolysis conditions and in the manner in which the ingredients are prepared for pyrolysis. In addition, one has an option to form QDs of controlled size without or with capping. Unlike in the prior process, one does not rely on formulation and pyrolysis process conditions to cause the QDs to form spontaneously in the desired size range. Instead, one forces the QDs to form in a desired relatively narrow size range by spraying a solution of QD-precursor material through an ultrasonic nozzle to form drops of controlled size. The average size of the drops can be tailored via the surface tension and density of the solution. Even more conveniently, the average size can be tailored via the frequency of ultrasonic agitation. Experiments have shown that for a given formulation, the average size is inversely proportional to frequency to the 2/3 power.

The basic concept of the improved process admits of variations. For example, in a simple embodiment of the process for making non-capped QDs, a precursor solution is sprayed into a cold-wall reactor that contains a substrate that is electrically heated to the desired reaction temperature (see figure). The drops falling on the substrate become pyrolyzed into QDs. In a slightly more complex example, capped QDs are made by similar spraying of a precursor solution into a hot passivating solvent.

This work was done by Kulbinder Banger, Michael H. Jin, and Aloysius Hepp of Glenn Research Center. Further information is contained in a TSP (see page 1).

Inquiries concerning rights for the commercial use of this invention should be addressed to NASA Glenn Research Center, Commercial Technology Office, Attn: Steve Fedor, Mail Stop 4-8, 21000 Brookpark Road, Cleveland, Ohio 44135. Refer to LEW-17444.



Mobile Robot for Exploring Cold Liquid/Solid Environments

This tethered robot could float, swim, crawl, and sample environmental materials.

NASA's Jet Propulsion Laboratory, Pasadena, California

The Planetary Autonomous Amphibious Robotic Vehicle (PAARV), now at the prototype stage of development, was originally intended for use in acquiring and analyzing samples of solid, liquid, and gaseous materials in cold environments on the shores and surfaces, and at shallow depths below the surfaces, of lakes and oceans on remote planets. The PAARV also could be adapted for use on Earth in similar exploration of cold environments in and near Arctic and Antarctic oceans and glacial and sub-glacial lakes.

The PAARV design is based partly on the design of prior ice-penetrating exploratory robots and partly on the designs of drop sondes heretofore used on Earth for scientific and military purposes. Like a sonde, the PAARV is designed to be connected to a carrier vehicle (e.g., a balloon, aircraft, or vessel in a terrestrial setting) by a tether, through which the carrier vehicle would provide power and would relay data communications between the PAARV and an external or remote control station. Like a sonde, the PAARV could be lowered from the carrier vehicle into an ocean or lake environment to be explored. Unlike a sonde, the PAARV would be capable of swimming and of crawling along the bottom, and crawling out of the ocean or lake and moving to a designated site of scientific interest on the shore.

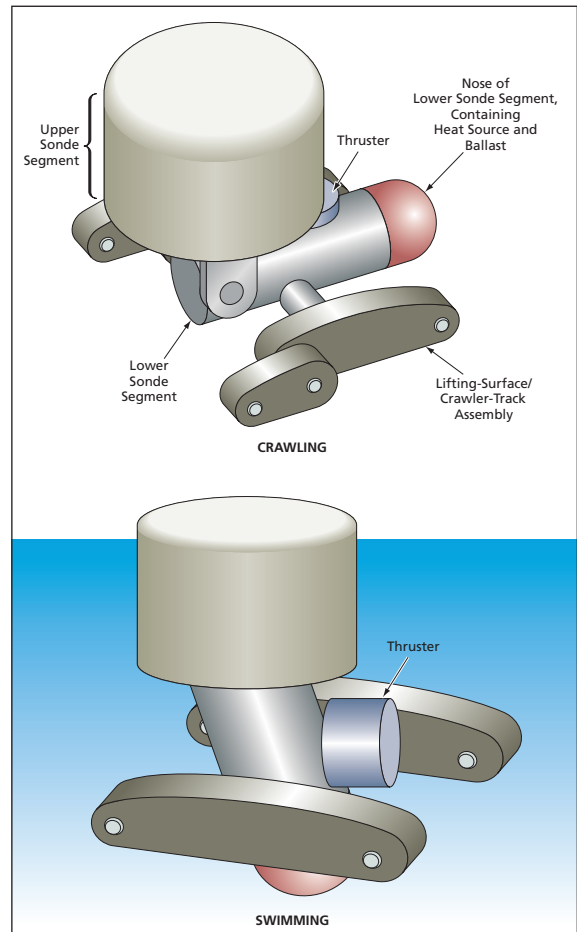
As now envisioned, the fully developed PAARV (see figure) would include an upper sonde segment and a lower sonde segment. Protruding from the lower sonde segment would be two assemblies containing both lifting surfaces (for control of attitude during descent and swimming) and crawler tracks. These assemblies could be rotated to align them parallel, perpendicular, or at an oblique angle with respect to the longitudinal axis of the lower sonde segment. Also protruding from the lower sonde segment, at a point above the center of gravity, would be a thruster for swimming.

The upper sonde segment would be cylindrical, approximately 30 cm in diam-

eter and 20 cm high. This segment would contain a tether-management-and-actuation subsystem; buoyancy-control chambers; a subsystem of pumps, actuators, and valves; a chamber holding compressed gas; and a chamber containing a heater. The upper sonde segment would be attached to the lower sonde segment via a single-joint actuator that effects rotation about an axis perpendicular to the longitudinal axes of the sonde segments.

The lower sonde segment would be approximately 60 cm long and 15 cm in diameter. Either a general-purpose radioisotope heat source or a mass of phase-change heat-storage material would be located in the nose (lower and outer end) of the lower sonde segment to keep instruments warm in the cold environment. The sonde would have a dual-walled shell with insulation to reduce the loss of heat. The heat source in the nose also would serve as ballast to maintain stability like that of a traditional ocean buoy.

When the PAARV was initially lowered from the carrier vehicle, the upper and lower sonde segments and the lifting-surface/crawler-track assemblies would be aligned collinearly so that the PAARV would float in a nominal vertical orientation like a buoy. Once the buoyancy chambers started to fill, the tether would be paid out from the top sonde segment of the PAARV descended. Upon arrival at a depth designated for swimming, the thruster would be activated and relative alignments of the upper and lower sonde segments and the lifting-surface/crawler-track assemblies varied as needed for steering. Upon contact with



The PAARV is shown here in two of its many possible crawling and swimming configurations.

the bottom, the lower sonde segment and the lifting-surface/crawler-track assemblies would be turned to a nominally horizontal orientation with the upper sonde segment in a nominally vertical orientation, and the crawler tracks would then be activated.

A sampling needle could be extended from the lower side of the lower sonde segment into the bottom of the ocean or lake, where it would adsorb bottom material. The needle would then be retracted, then heated to desorb the material for analysis by instruments in the lower sonde segment. The data from the analyses would be relayed to the external control station via the tether.

Once the bottom sampling was complete, the PAARV would increase its buoyancy by displacing liquid from the buoyancy-control chambers and would reel the tether back in. An onboard guidance, navigation, and control system coupled with acoustic range sensors would enable the vehicle to move slowly

toward shore as it ascended. Upon contact with ascending slope, the crawler tracks would be rotated to the angle of the slope and the crawler tracks would be activated. Once out of the water, the PAARV would crawl to a location of interest designated by coordinates provided by cameras on the carrier vehicle

or an aircraft overhead. The sampling process would be repeated at the location of interest.

This work was done by Charles Bergh and Wayne Zimmerman of Caltech for NASA's Jet Propulsion Laboratory. Further information is contained in a TSP (see page 1) NPO-40731

System Would Acquire Core and Powder Samples of Rocks

A sampling system would be built around an ultrasonic/sonic drill corer.

NASA's Jet Propulsion Laboratory, Pasadena, California

A system for automated sampling of rocks, ice, and similar hard materials at and immediately below the surface of the ground is undergoing development. The system, denoted a sample preparation, acquisition, handling, and delivery (SPAHD) device, would be mounted on a robotic exploratory vehicle that would traverse the terrain of interest on the Earth or on a remote planet. The SPAHD device would probe the ground to obtain data for optimization of sampling, prepare the surface, acquire samples in the form(s) of cores and/or powdered cuttings, and deliver the samples to a selected location for analysis and/or storage.

The SPAHD device would be built around an ultrasonic/sonic drill corer (USDC) — an apparatus that was reported in “Ultrasonic/Sonic Drill/Corers With Integrated Sensors” (NPO-20856), *NASA Tech Briefs*, Vol. 25, No. 1 (January 2001), page 38. To recapitulate: A USDC includes a hollow drill bit or corer, in which combinations of ultrasonic and sonic vibrations are excited by an electronically driven piezoelectric actuator. The corer can be instrumented with a variety of sensors (and/or the drill bit or corer can be used as an acoustic-impedance sensor) for both probing the drilled material and acquiring feedback for control of the excitation. The USDC advances into the material of interest by means of a hammering action and a resulting chiseling action at the tip of the corer. The hammering and chiseling actions are so effective that unlike in conventional twist drilling, a negligible amount of axial force is needed to make the USDC advance into the material. Also unlike a conventional twist drill, the USDC operates without need for torsional restraint, lubricant, or a sharp bit.

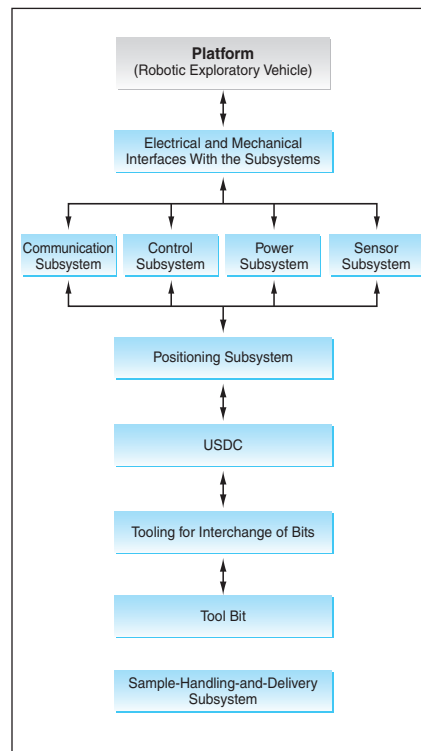


Figure 1. A SPAHD Device would be a highly integrated system containing specially designed mechanisms and electronic circuits working together to perform multiple functions, including probing, preparation of surfaces, acquisition of core and powder samples, and manipulation and delivery of the samples. The relative positions in this block diagram indicate approximate mechanical and electrical relationships among subsystems and components.

In addition to a USDC, the SPAHD device (see Figure 1) would include sensor, control, and communication subsystems; a subsystem for positioning the USDC at the desired position and orientation on the ground; a set of interchangeable USDC bits; a tool rack to store the bits; and mechanisms for manipulating and delivering samples. The

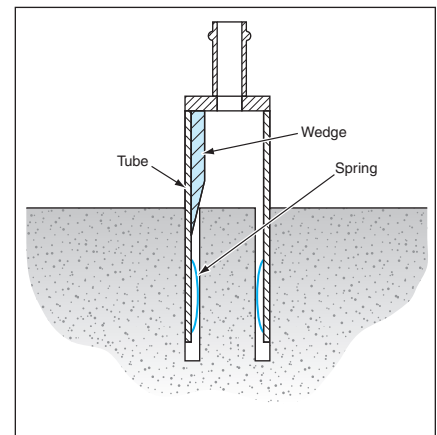


Figure 2. An Extraction Bit is one example of special-purpose bits that would be included in a SPAHD device. This bit would be inserted around a recently cut core. The wedge in the bit would introduce a transverse force that would cause the core to break off somewhere near its root. The springs in the bit would then retain the core so that the core could be lifted out of the hole.

bits would be attached to, and detached from, a resonator horn of the piezoelectric actuator by means of simple-to-operate snap-on/snap-off mechanisms. The set of bits would include a probing bit, bits for cutting cores and collecting powdered cuttings, bits for extracting the cores after they have been cut (see Figure 2), and an ultrasonic rock abrasion tool (URAT) bit [described in “Ultrasonically Actuated Tools for Abrading Rock Surfaces” (NPO-30403), *NASA Tech Briefs*, Vol. 30, No. 7 (July, 2006), page 58.

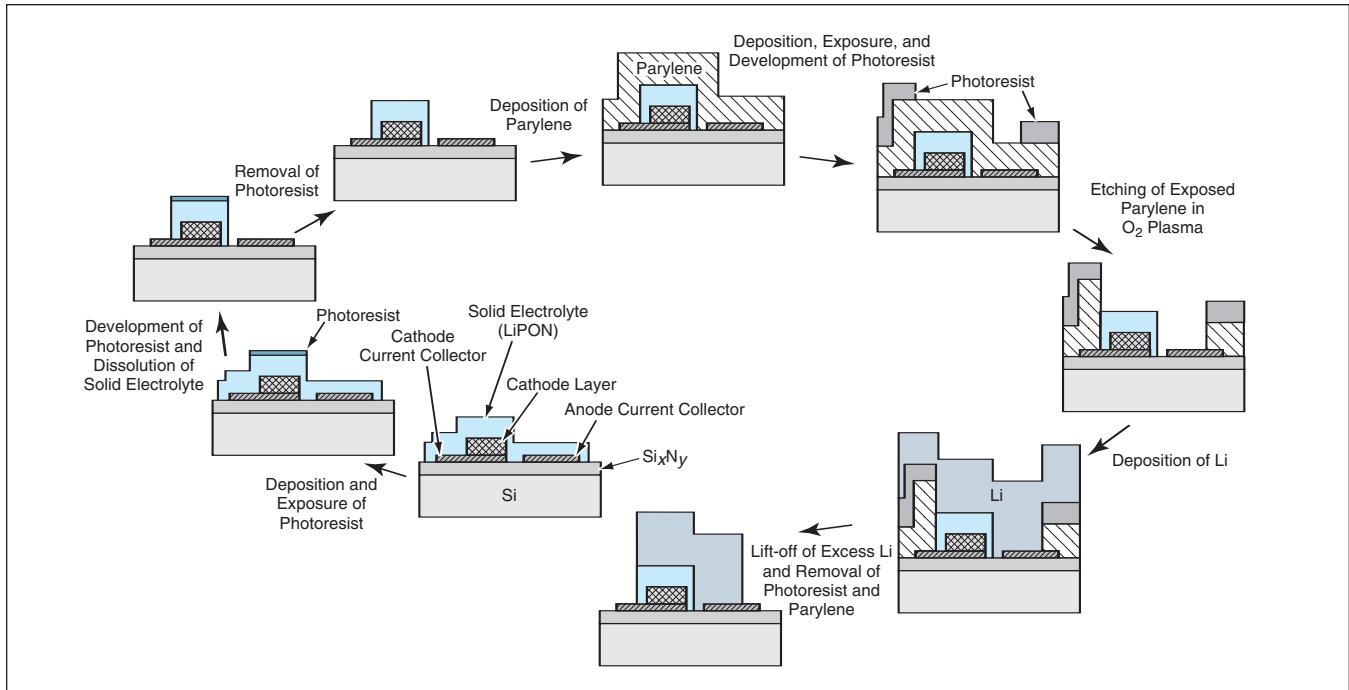
This work was done by Yoseph Bar-Cohen, James Randolph, Xiaqi Bao, Stewart Sherit, Chuck Ritz, and Greg Cook of Caltech for NASA's Jet Propulsion Laboratory. Further information is contained in a TSP (see page 1). NPO-30640



Improved Fabrication of Lithium Films Having Micron Features

Dry chemicals and a dry process are used to prevent undesired reactions.

NASA's Jet Propulsion Laboratory, Pasadena, California



A Lithium Anode in a Microelectrochemical Cell is fabricated in a dry process.

An improved method has been devised for fabricating micron-dimension Li features. This approach is intended for application in the fabrication of lithium-based microelectrochemical devices — particularly solid-state thin-film lithium microbatteries.

The need for this special process arises because lithium engages in undesired chemical reactions with water and with most of the chemicals commonly used in the microfabrication of silicon and other materials. The method described below involves the use of only water-free “dry” chemicals that are compatible with lithium. The figure illustrates the pertinent steps in the fabrication of a microelectrochemical cell containing a lithium anode.

The following steps are performed in sequence:

1. The solid-electrolyte layer is covered with AZ 1518 (or equivalent) photoresist, which is then exposed to ultraviolet light in a pattern that defines the areas from which the solid electrolyte is to be removed.

2. The photoresist developer dissolves both the photoresist and the underlying solid electrolyte from the aforementioned areas, leaving developed photoresist and underlying solid electrolyte only in a defined area.
3. The developed photoresist is removed by use of dry acetone, leaving the solid electrolyte in the defined area.
4. A layer of parylene 2 to 4 μm thick is deposited over the entire workpiece.
5. NR 5-8000 (or equivalent) photoresist is applied, exposed, and developed. The opening between areas covered by developed photoresist defines the anode area on which lithium is to be deposited.
6. The exposed parylene is etched away in oxygen plasma.
7. A thin film of lithium is evaporatively deposited on the workpiece.
8. Adhesive tape (Kapton, or equivalent) is pressed onto the top of the workpiece, then pulled off. The lithium deposited on the photoresist-covered areas adheres more weakly than does the lithium deposited on the anode

area, to such a degree that pulling off the tape removes all lithium from covering the photoresist while leaving all the lithium in the desired anode area.

9. The photoresist and the remaining parylene are removed by use of dry acetone and subsequent etching in oxygen plasma.

This work was done by Jay Whitacre and William West of Caltech for NASA's Jet Propulsion Laboratory. Further information is contained in a TSP (see page 1).

In accordance with Public Law 96-517, the contractor has elected to retain title to this invention. Inquiries concerning rights for its commercial use should be addressed to:
Innovative Technology Assets Management
JPL
Mail Stop 202-233
4800 Oak Grove Drive
Pasadena, CA 91109-8099
(818) 354-2240

E-mail: iaoffice@jpl.nasa.gov
Refer to NPO-30725, volume and number of this NASA Tech Briefs issue, and the page number.

Manufacture of Regularly Shaped Sol-Gel Pellets

For mass production, an extrusion process is superior to a spray process.

John H. Glenn Research Center, Cleveland, Ohio

An extrusion batch process for manufacturing regularly shaped sol-gel pellets has been devised as an improved alternative to a spray process that yields irregularly shaped pellets. The aspect ratio of regularly shaped pellets can be controlled more easily, while regularly shaped pellets pack more efficiently. In the extrusion process, a wet gel is pushed out of a mold and chopped repetitively into short, cylindrical pieces as it emerges from the mold. The pieces are collected and can be either (1) dried at ambient pressure to xerogel, (2) solvent exchanged and dried under ambient pressure to ambigels, or (3) supercritically dried to aerogel. Advantageously, the extruded pellets can be dropped directly in a cross-linking bath, where they develop a conformal polymer coating around the skeletal framework of the wet gel via reaction with the cross linker. These pellets can be dried to mechanically robust X-Aerogel.

The extrusion process begins with the preparation of a suitable sol. This is accomplished online by mixing two solutions as they flow from two separate containers towards the mold. A typical sol that yields a gel that can be cross-linked easily is made by mixing two cold solu-

tions: One solution consists of 4.5 volume parts of acetonitrile, 0.482 volume parts of aminopropyltriethoxysilane, and 1.45 volume parts of tetramethoxysilane. The other solution consists of 4.5 volume parts of acetonitrile and 1.5 volume parts of water.

The cold sol is equipped with a plunger. As soon as the sol gels in the mold, the newly formed gel is pushed out of the mold and is chopped to the desired length. When the gel mold is exhausted, the plunger is retracted and the process repeated. An important consideration in the process is that the sol needs to have formed a gel, which is stable enough to slice before the extrusion process is begun. The process can be used with nearly any sol-gel formulations, but high throughout requires a fast gelling sol such as the one obtained by using aminopropyltriethoxysilane (APTES)/tetramethoxysilane (TMOS) mixtures. In this formulation, control of the gelation rate requires that the precursor solutions must be refrigerated prior to filling the mold. In an extension of the basic process described here, multiple molds with plungers can be connected to a liquid manifold con-

nected to a sol-preparation apparatus and mounted together to facilitate repeated filling with sol and automatic extrusion.

The most benefit from this process is realized when it is combined with chemical cross linking as pellets emerge from the mold. A suitable cross linker is a diisocyanate (e.g., Desmodour N3200 from Bayer Corporations, or equivalent), which, owing to the small size of the pellets, diffuses and reacts quickly with the internal surfaces of the porous nanoparticle framework of the wet gels. The wet-pellets are subsequently dried from supercritical carbon dioxide, yielding mechanically robust colorless, slightly translucent pellets of X-Aerogel. Other cross-linker systems such as epoxies and polyolefins have been also investigated.

This work was done by Nicholas Leventis, James C. Johnston, and James D. Kinder of Glenn Research Center. Further information is contained in a TSP (see page 1)

Inquiries concerning rights for the commercial use of this invention should be addressed to NASA Glenn Research Center, Innovative Partnerships Office, Attn: Steve Fedor, Mail Stop 4-8, 21000 Brookpark Road, Cleveland, Ohio 44135. Refer to LEW-17787-1.



Regulating Glucose and pH, and Monitoring Oxygen in a Bioreactor

Glucose and oxygen concentrations are monitored, and glucose concentration and pH are adjusted as needed.

Lyndon B. Johnson Space Center, Houston, Texas

Figure 1 is a simplified schematic diagram of a system that automatically regulates the concentration of glucose or pH in a liquid culture medium that is circulated through a rotating-wall perfused bioreactor. Another system, shown in Figure 2, monitors the concentration of oxygen in the culture medium.

The glucose-regulating system includes an electrochemical sensor that measures the concentration of glucose in the medium flowing out of the bioreactor, a reservoir containing a concentrated glucose stock solution, and a peristaltic pump. The sensor reading is digitized and monitored by a computer, which generates commands to open and close valves, as described below, to adjust the concentration of glucose. This allows the system to maintain an optimal concentration of glucose without using large volumes of cell culture medium. The glucose control system operates in one of the following three modes (see Figure 1): perfusion, where the medium is simply circulated without adding or removing any liquid; infusion, where fresh

cell medium is introduced into circulation, replacing the spent medium in the bioreactor; injection, where a small amount of concentrated glucose solution is added to the bioreactor when the glucose concentration falls below 75 mg/dL.

The electrochemical glucose sensor includes a membrane that is covered with a thin (10 to 200 nm thick) layer of immobilized glucose oxidase enzyme and is coupled to a three-electrode amperometric probe and a flow cell. Glucose diffuses through the membrane and, in the presence of the glucose oxidase, is converted to hydrogen peroxide and gluconic acid. The rate of generation of hydrogen peroxide is measured amperometrically on a platinum working electrode at a potential of 0.7 V with respect to an Ag/AgCl reference electrode. The sensor reading is correlated with the concentration of glucose by the Michaelis-Menten equation,

$$I = I_{\max}S / (K + S),$$

where I is the sensor current, I_{\max} is the maximum sensor current for the amper-

ometric reaction, K is a constant, and S is the concentration of glucose. The constants I_{\max} and K are determined by means of a two-point calibration, using a commercial glucose analyzer to determine the glucose concentrations. This sensor system has been tested in cell culture experiments for over 50 days. The control of glucose in this manner reduces the amount of culture medium required to optimally grow cells.

The pH sensor, described in "Optoelectronic Instrument Monitors pH in a Culture Medium" (MSC-23107), NASA Tech Briefs, Vol. 28, No. 9 (September 2004), page 4a, was coupled to the above control system containing a small volume of a mixture of sodium and potassium hydroxide and bicarbonate solution to form a pH control system. When the sensor pH output fell below a preset level, a small amount of buffer was injected to the bioreactor to bring the pH to the desired level. This system was tested in a 120-day cell run, where the pH was controlled at 7.1 ± 0.1 pH unit. The volume of buffer used was negligible compared to the volume of cell culture medium required for the same level of pH control. By controlling the culture pH in this manner, the cells produced less biofilm.

The oxygen-monitoring system is designed to satisfy special requirements for noninvasiveness, sterilizability, compactness, light weight, and nontoxicity to the cells nourished by the solution. The oxygen sensor exploits dynamic quenching of fluorescence by oxygen molecules. The sensor includes a capillary tube of inside diameter 2 mm, lined with a 0.1-mm-thick sensing layer of oxygen-sensitive fluorescent dye, and titanium oxide encapsulated in a gas-permeable, ion-impermeable silicone rubber. The sensing layer is overlaid with a black shielding layer of carbon black encapsulated in silicone rubber. The solution of interest flows through the tube, and oxygen from the solution permeates the silicone-rubber layers. The degree of permeation

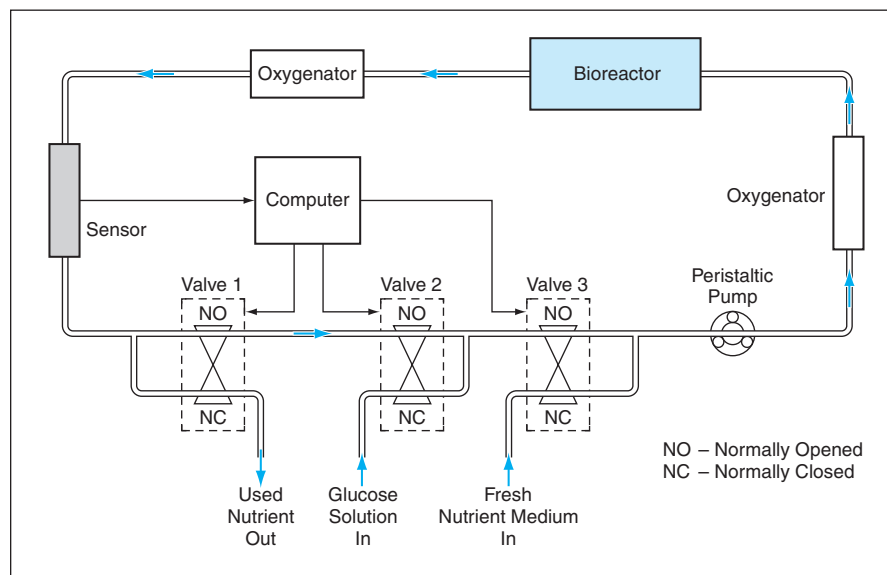


Figure 1. Valves Are Momentarily Switched between open and closed positions, to inject concentrated glucose solution and drain used nutrient medium, when the measured concentration of glucose in the circulating nutrient medium falls to a preset minimum level.

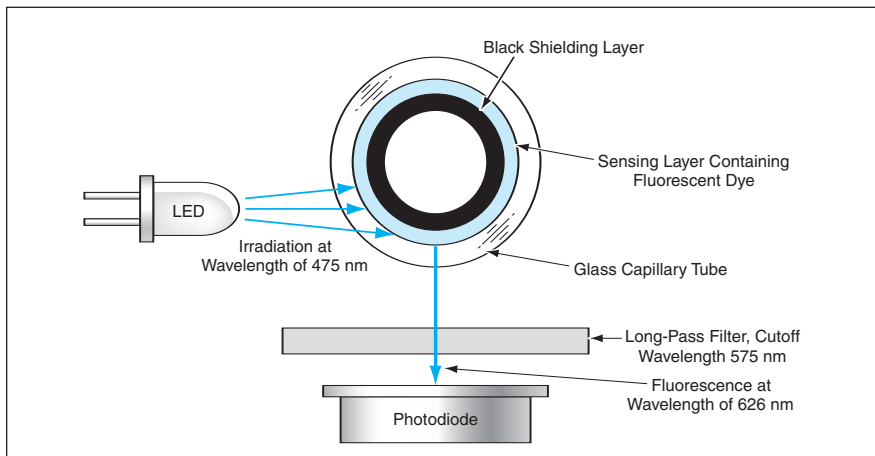


Figure 2. Blue Light From the LED excites red fluorescence in the dye encapsulated in the silicone rubber. The intensity of the fluorescence, measured by use of the photodiode, varies with the concentration of oxygen dissolved in the solution flowing through the tube.

(and, hence, the rate of quenching of fluorescence) is reversible; that is, it varies along with the concentration of dissolved oxygen.

The dye is tris(4,7-diphenyl-1,10-phenanthroline)ruthenium(II)chloride $[\text{Ru}(\text{dpp})_3\text{Cl}_2]$, which exhibits a high quantum yield (30 percent) of red (wavelength 626 nm) fluorescence with a lifetime of 5.34 ms after irradiation with blue light. A pulsed light-emitting diode (LED) of wavelength 465 nm is used as the radiation source. Operation in pulse mode minimizes the dye-bleach-

ing effect that could occur if the LED were to irradiate the dye continuously during long-term monitoring. A long-wavelength-pass filter is used to remove the blue LED light reflected and scattered by the irradiated capillary tube and its contents. The remaining light — predominantly the red fluorescence — is detected by a photodiode.

The pulsed output of the photodiode is digitized and processed to determine the concentration of dissolved oxygen in terms of the partial pressure of oxygen ($p\text{O}_2$). This determination is made by

use of the Stern-Volmer equation for the intensity and fluorescence lifetime of oxygen-quenched fluorescence of a luminescent dye:

$$I_0/I = \tau_0/\tau = 1 + K_{sv}(p\text{O}_2),$$

where I_0 and I are the intensities of fluorescence in the absence and presence of oxygen, respectively; τ_0 and τ are the fluorescence-decay lifetimes in the absence and presence of oxygen, respectively; and K_{sv} (the Stern-Volmer constant) depends on details of the sensor design and construction. The sensor is calibrated by use of a phosphate-buffered saline solution containing a known elevated concentration of oxygen. The oxygen sensor was tested for over 180 days in a perfused rotating-wall bioreactor, using a single, initial calibration for the entire experiment.

This work was done by Melody M. Anderson and Neat R. Pellis of Johnson Space Center, and Antony S. Jeevarajan, Thomas D. Taylor, Yuanhang Xu, Frank Gao of Wyle Laboratories. For further information, contact the Johnson Innovative Technology Partnerships Office at (281) 483-3809.

This invention is owned by NASA, and a patent application has been filed. Inquiries concerning nonexclusive or exclusive license for its commercial development should be addressed to the Patent Counsel, Johnson Space Center, (281) 483-0837. Refer to MSC-23473/504/13/54.



Satellite Multiangle Spectropolarimetric Imaging of Aerosols

One instrument would implement a synergistic combination of multispectral, multiangle, and polarimetric techniques.

NASA's Jet Propulsion Laboratory, Pasadena, California

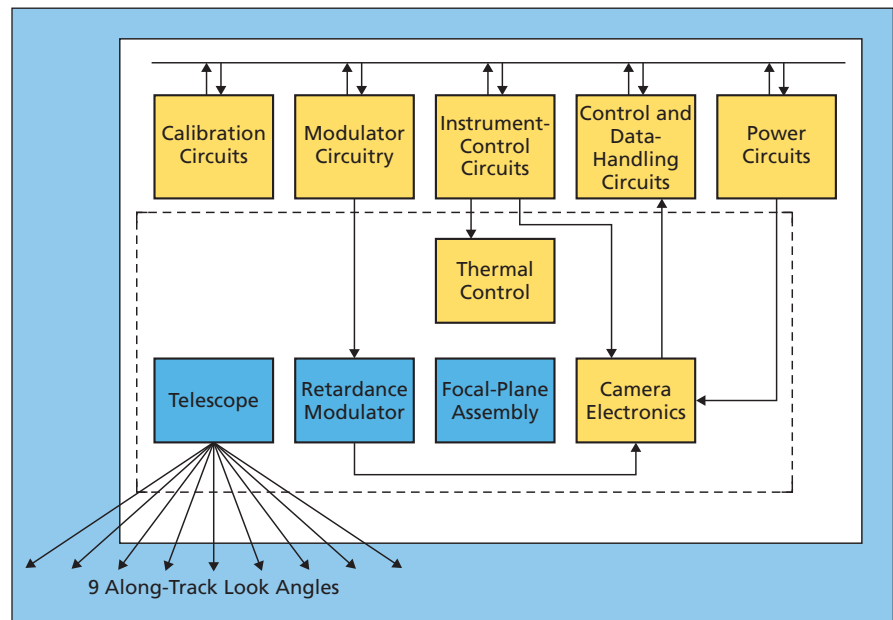
A proposed remote-sensing instrument, to be carried aboard a spacecraft in orbit around the Earth, would gather data on the spatial distribution and radiative characteristics of tropospheric aerosols. These data are needed for better understanding of the natural and anthropogenic origins of aerosols, and of the effects of aerosols on climate and atmospheric chemistry.

The instrument would implement a synergistic combination of multispectral, multiangle, and polarimetric measurement techniques to increase the accuracies of aerosol-optical-depth and aerosol-particle-property characterizations beyond what is achievable by use of each technique by itself. Additional benefits expected to be realized by the specific novel combination of different measurement techniques in one instrument include the following:

- The instrument could make simultaneous measurements (described below) that are essential for determining the mesoscale variability of aerosols;
- The instrument would have a wide-swath, high-resolution imaging capability for discerning clouds and for frequent global sampling; and
- The cost of building this instrument would be less than the cost of building separate instruments for the various measurements.

Features of the design and performance of the instrument would include spectral coverage from near ultraviolet to short-wave infrared, global spatial coverage within a few days, simultaneous intensity and polarimetric imaging at multiple view angles, kilometer to sub-kilometer spatial resolution, and measurement of the degree of linear polarization in one visible and one short-wave infrared spectral band.

The instrument (see block diagram) would acquire data in push-broom fashion in nine cross-ground-track swaths, each aimed at a different along-ground-track look angle. A separate camera would be used for each



This **Simplified Block Diagram** shows the functional relationships among basic components of the proposed instrument.

look angle, but all nine cameras could be of the same design. Reflective telescope and camera optics would be used because they offer significant advantages over refractive optics, including high transmittance over the broad wavelength range of interest, absence of chromatic aberration, the possibility of achieving the desired effects by use of fewer optical elements, less susceptibility to formation of ghost images, and better and more stable polarization performance. The instrument would measure intensity at wavelengths of 380, 412, 446, 558, 866, 1,375, and 2,130 nm. Polarization plus intensity would be measured at 670 and 1,630 nm.

The design of the instrument would be dominated by the requirement for polarimetric accuracy. Of several polarimetric approaches that were considered, the one selected to satisfy this requirement involves adaptation of advanced techniques of high-precision imaging polarimetry used in ground-based solar astronomy. The approach

involves the use of (1) a photoelastic modulator to rapidly rotate the plane of polarization, (2) one or two analyzers and corresponding linear arrays of photodetectors, and (3) demodulation of the photodetector outputs to obtain data from which one can compute the Stokes parameters Q and U (pertaining to the predominance of horizontal over vertical linear polarization and the predominance of 45° over 135° polarization, respectively). In order to implement the specific detection scheme, it would be necessary to design and build flight-qualified modulators, as well as a custom complementary metal oxide/semiconductor integrated circuit for the low-noise, rapid-readout photodetector array.

This work was done by David Diner, Steven Macenka, Lawrence Scherr, and Suresh Seshadri of Caltech; Russell Chipman of the University of Arizona; and Christoph Keller of the National Solar Observatory for NASA's Jet Propulsion Laboratory. Further information is contained in a TSP (see page 1). NPO-40936

Interferometric System for Measuring Thickness of Sea Ice

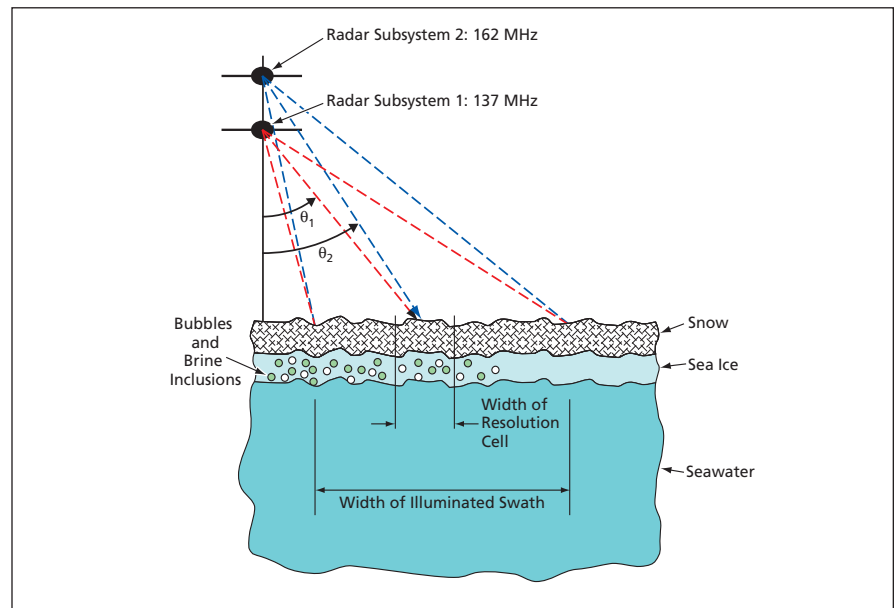
Frequency- and spatial-domain VHF radar interferometry are used.

NASA's Jet Propulsion Laboratory, Pasadena, California

The cryospheric advanced sensor (CAS) is a developmental airborne (and, potentially, spaceborne) radar-based instrumentation system for measuring and mapping the thickness of sea ice. A planned future version of the system would also provide data on the thickness of snow covering sea ice. Frequent measurements of the thickness of polar ocean sea ice and its snow cover on a synoptic scale are critical to understanding global climate change and ocean circulation.

The CAS system includes two relatively-narrow-band chirped radar subsystems that operate about two different nominal middle frequencies in the very-high-frequency (VHF) range (e.g., 137 and 162 MHz). The radar targets the same surface area from two slightly different directions (see figure). The radar backscatter signals are processed to extract angular- and frequency-domain correlation functions (ACF/FCF) so that the system acts, in effect, as a combined spatial- and frequency-domain interferometric radar system.

The phase of the ACF/FCF varies with the thickness of the sea ice. To enable the utilization of the phase information to compute this thickness, the interactions between the radar waves and the seawater, ice, and snow cover are represented by a mathematical model: The snow, sea ice (including air bubbles and brine inclusions), and seawater are represented as layers, each characterized by an assumed thickness and a known or assumed complex-number index of refraction. Each interface (air/snow, snow/ice, and ice/water) is modeled as deviating from a plane by a surface roughness



Two Chirped VHF Radar Subsystems operating about different nominal middle frequencies targets the same surface area from two slightly different angles. Frequency- and spatial-domain interferometric computations performed on the radar backscatter signals enable determination of the thickness of the sea ice.

characterized by a Gaussian spectrum. The scattering of the radar waves from the interfaces is computed by use of small-perturbation and Kirchhoff rough-surface submodels. The scattering from within the layers is computed by a Rayleigh volume scattering model. The ACF/FCF is computed from the scattered signals.

Assuming that the ACF/FCF obeys the model, the interferometric phase information can be inverted by use of a suitable computational inversion technique (e.g., a genetic algorithm or gradient descent or other least-squares technique) to obtain the thickness of the sea ice. In essence, the inversion amounts to seek-

ing whichever value of sea-ice thickness used in the model yields the best match between (1) the ACF/FCF interferometric phase computed from the model and (2) the ACF/FCF measured interferometric phase.

This work was done by Ziad Hussein, Rolando Jordan, Kyle McDonald, Benjamin Holt, and John Huang of Caltech; Yasuo Kugo, Akira Ishimaru, and Sermsak Jaruwatanadilok of the University of Washington, Seattle; and Torry Akins and Prasad Gogineni of the University of Kansas, Lawrence, for NASA's Jet Propulsion Laboratory. Further information is contained in a TSP (see page 1). NPO-42391

Microscale Regenerative Heat Exchanger

Materials and dimensions are chosen to optimize performance at microscale.

John H. Glenn Research Center, Cleveland, Ohio

The device illustrated in Figure 1 is designed primarily for use as a regenerative heat exchanger in a miniature Stirling engine or Stirling-cycle heat pump. A regenerative heat exchanger (sometimes called, simply, a "regenerator" in

the Stirling-engine art) is basically a thermal capacitor: Its role in the Stirling cycle is to alternately accept heat from, then deliver heat to, an oscillating flow of a working fluid between compression and expansion volumes, without intro-

ducing an excessive pressure drop. These volumes are at different temperatures, and conduction of heat between these volumes is undesirable because it reduces the energy-conversion efficiency of the Stirling cycle. Hence, among the

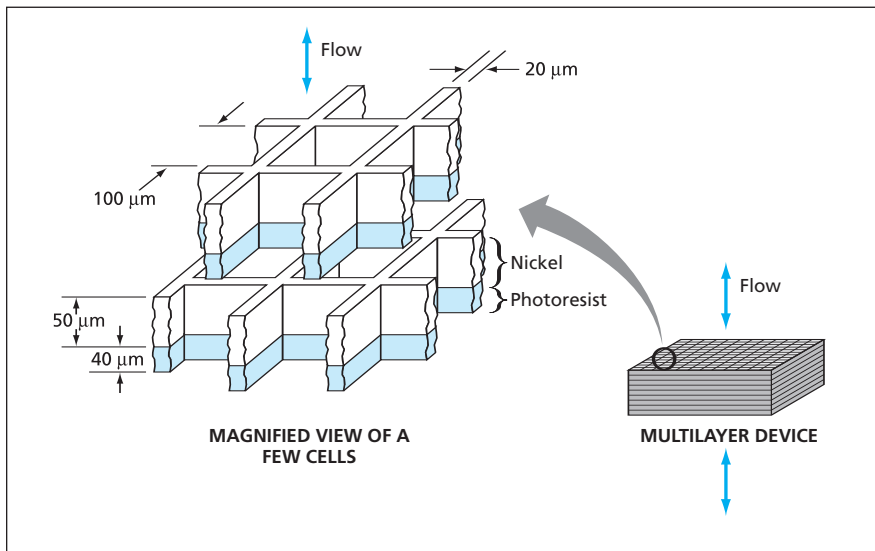


Figure 1. The Configuration of This Device Is Typical of a microscale heat exchanger as described in the text. The materials and dimensions shown here are representative rather than exclusive: they were chosen in a design trade study in which account was taken of capabilities for fabrication and of requirements for low axial thermal conduction and low pressure drop under a specific set of assumptions.

desired characteristics of a regenerative heat exchanger are low pressure drop and low thermal conductivity along the flow axis.

As shown in the enlarged views in Figure 1, the device features a multilayer grating structure in which each layer is offset from the adjacent layer by half a cell opening along both axes perpendicular to the flow axis. In addition, each grating layer is a composite of a high-thermal conductivity (in this case, nickel) sublayer (see Figure 2) and a low-thermal-conductivity (in this case, photoresist) sublayer. As a hot fluid flows through from, say, top to bottom, heat from the fluid is transferred to, and stored in, the cell walls of this de-

vice. Next, when cold fluid flows from bottom to top, heat is transferred from the cell walls to the fluid.

Axial thermal conduction in such a device can be minimized by constructing it of many layers containing low-thermal-conductivity sublayers. The offset of adjacent layers creates reduced-size, partially isolated cross sections for thermal conduction, thereby further reducing the overall axial thermal conductance of the device.

Once the device has been installed in its intended operational setting (e.g., as a regenerative heat exchanger in a Stirling machine), some delamination of the layers is permissible, provided that the half-cell offset between

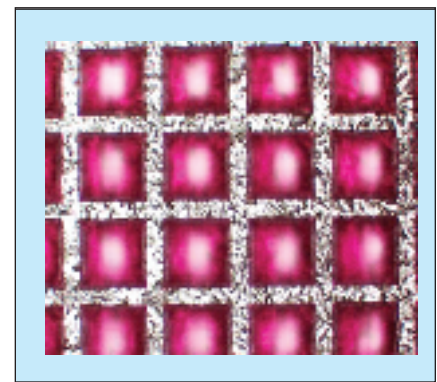


Figure 2. A Microphotograph of a portion of one layer of the fabricated microscale heat exchanger shows the grating structure and surface features of the nickel sublayer.

adjacent layers is maintained and no debris is produced. Indeed, delamination enhances performance by reducing axial thermal conduction.

The reasonably high porosity of the device helps to keep the pressure drop low. The layer-to-layer offset disrupts the formation of boundary layers in the flow, thereby contributing to the maintenance of low pressure drop. Disruption of boundary layers also increases the coefficient of transfer of heat between the fluid and the cell walls.

This work was done by Matthew E. Moran of Glenn Research Center, and Stephan Stelter and Manfred Stelter of Polar Thermal Technologies. Further information is contained in a TSP (see page 1).

Inquiries concerning rights for the commercial use of this invention should be addressed to NASA Glenn Research Center, Commercial Technology Office, Attn: Steve Fedor, Mail Stop 4-8, 21000 Brookpark Road, Cleveland, Ohio 44135. Refer to LEW-17526-1.



Protocols for Handling Messages Between Simulation Computers

Both time-critical and delivery-critical characteristics are accommodated.

Lyndon B. Johnson Space Center, Houston, Texas

Practical Simulator Network (PSimNet) is a set of data-communication protocols designed especially for use in handling messages between computers that are engaging cooperatively in real-time or nearly-real-time training simulations. In a typical application, computers that provide individualized training at widely dispersed locations would communicate, by use of PSimNet, with a central host computer that would provide a common computational-simulation environment and common data. Originally intended for use in supporting interfaces between training computers and computers that simulate the responses of spacecraft scientific payloads, PSimNet could be especially well suited for a variety of other applications — for example, group automobile-driver training in a classroom. Another potential application might lie in networking of automobile-diagnostic computers at repair facilities to a central computer that would compile the expertise of numerous technicians and engineers and act as an expert consulting technician.

Heretofore, a message transported in a data-communication network has been of one of two types: delivery-critical or time-

critical. Networks that transport delivery-critical messages need protocols that assure the sending computers that delivery-critical messages are in fact delivered to the proper recipient computers. Networks that transport time-critical messages need protocols that deliver messages to the intended recipient computers as quickly as possible because the value of a time-critical message diminishes over time. (Typically, it is better to send an updated time-critical message than to time out and resend a stale time-critical message.) Prior to the conception of PSimNet, there was no available set of protocols that would enable a network to handle both time-critical and delivery-critical messages.

PSimNet is built on the Transmission Control Protocol/ Internet Protocol (TCP/IP) suite of protocols, which includes the TCP and the user datagram protocol (UDP). The TCP/IP and the UDP protocols offer offsetting advantages and disadvantages with respect to the reliability needed for transport of delivery-critical messages and the speed needed for transport of time-critical messages: TCP/IP provides some assurances of proper delivery of a delivery-critical mes-

sage, but at the cost of some overhead. UDP does not offer such assurances, but offers greater efficiency, which is an advantage for delivering time-critical messages.

The figure depicts the relationships among the hardware and software subsystems and a message in a data-communication system that uses PSimNet. The overall function of the system is to convey a message from the first computer to a second computer. The message begins with a header that, among other things, specifies a delivery characteristic (time-critical or delivery-critical). First, the message is received by a message receiver, then its delivery characteristic is analyzed by a message-type determinator. On the basis of the analyzed delivery characteristic, a message-delivery selector then selects the protocol to be used in transporting the message. In the present version of PSimNet, the preferred protocol for time-critical messages is UDP, while that for delivery-critical messages is a modified version of UDP that incorporates additions to make it more reliable.

A message transporter then transports the message to the second computer by use of the selected protocol. The message transporter can send the message to multiple computers if instructed to do so by the first computer.

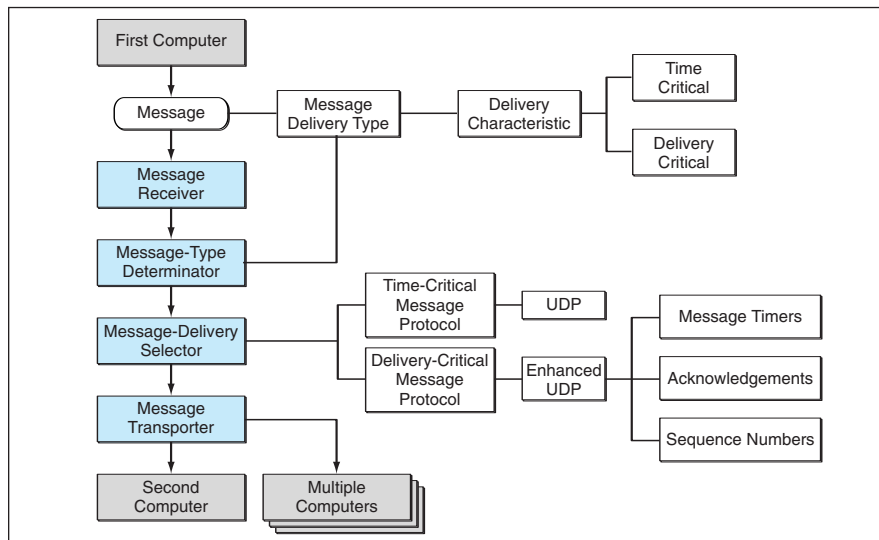
This work was done by John P. Balcerowski and Milton Dunnam of Hughes Electronics Corp. (now Raytheon Corp. Aerospace Engineering Services Division) for Johnson Space Center. Further information is contained in a TSP (see page 1).

Title to this invention, covered by U.S. Patent No. 6,101,545, has been waived under the provisions of the National Aeronautics and Space Act {42 U.S.C. 2457 (f)}. Inquiries concerning licenses for its commercial development should be addressed to:

*Hughes Electronics Corp.
200 N. Sepulveda Blvd.
P.O. Box 956*

El Segundo, CA 90245-0956

Refer to MSC-23147, volume and number of this NASA Tech Briefs issue, and the page number.



A Message Is Sent From One Computer to Another in a data-communication network that utilizes the PSimNet set of protocols. PSimNet makes it possible to handle both time-critical and delivery-critical messages in the same network.

▶ Statistical Detection of Atypical Aircraft Flights

A priori specification of search criteria is not necessary.

Ames Research Center, Moffett Field, California

A computational method and software to implement the method have been developed to sift through vast quantities of digital flight data to alert human analysts to aircraft flights that are statistically atypical in ways that signify that safety may be adversely affected. On a typical day, there are tens of thousands of flights in the United States and several times that number throughout the world. Depending on the specific aircraft design, the volume of data collected by sensors and flight recorders can range from a few dozen to several thousand parameters per second during a flight. Whereas these data have long been utilized in investigating crashes, the present method is oriented toward helping to prevent crashes by enabling routine monitoring of flight operations to identify portions of flights that may be of interest with respect to safety issues.

Experience has taught that statistically atypical flights often pose safety issues. Conventional methods of finding anomalous flights in bodies of digital flight data require users to pre-define the operational patterns that constitute unwanted performances. Typically, for example, a program examines flight data for exceedences (e.g., instances of excessive speed, excessive acceleration, and other parameters outside normal ranges). In other words, a conventional flight-data-analysis computer program finds only the patterns it is told to seek

in flight data, and is blind to newly emergent patterns that it has not been told to seek. The present method overcomes this deficiency in that it does not require any pre-specification of what to look for in bodies of flight data. The method is based partly on the principle that it is necessary, not only to look for exceedences, but to go beyond exceedences, looking for more subtle data patterns that often cannot be prescribed in advance.

The method involves a series of processing steps that convert the massive quantities of raw data, collected during routine flight operations, into useful information. The raw data are progressively reduced using both deterministic and statistical methods. Multivariate cluster analysis is performed to group flights by similarity with respect to flight signatures derived from parameter values. The process includes analysis of multiple selected flight parameters for a selected phase of a selected flight, and for determining when the selected phase of the selected flight is atypical in comparison with the corresponding phases of other, similar flights for which corresponding data are available. For each flight, there is computed an atypicality score based partly on results from the cluster analysis. The distribution of atypicality scores of all flights is used to identify flights for examination.

The data from each day's flights are processed during the night and sum-

marized in a document, called the "Morning Report," that includes a list of the 20 percent of flights having the highest atypicality scores, ranked in order of descending atypicality score. For each flight, the report includes a plain-language description of what makes the flight atypical. With the help of software designed to be intuitively useable, an analyst works through this list of flights to the finest level of detail where necessary, examining the characteristics that made them atypical, assessing their operational significance, and determining the need for further action.

This work was done by Irving Staller, Thomas Chidester, and Michael Shafto of Ames Research Center; Thomas Ferryman, Brett Amidan, Paul Whitney, Amanda White, Alan Willse, Scott Cooley, Joseph Jay, Loren Rosenthal, Andrea Swickard, Derrick Bates, Chad Scherrer, and Bobbie-Jo Webb of Battelle Memorial Institute; Robert Lawrence of Safe Flight; Chris Mosbrucker, Gary Prothero, Adi Andrei, Tim Romanowski, Daniel Robin, and Jason Prothero of ProWorks Corporation; Robert Lynch of Flight Safety Consultants; and Michael Lowe of the U.S. Navy. Further information is contained in a TSP (see page 1).

This invention has been patented by NASA (U.S. Patent No. 6,937,924). Inquiries concerning rights for the commercial use of this invention should be addressed to the Ames Technology Partnerships Division at (650) 604-2954. Refer to ARC-15041-1

▶ NASA's Aviation Safety and Modeling Project

Capabilities for automated analysis of flight data are under development.

Ames Research Center, Moffett Field, California

The Aviation Safety Monitoring and Modeling (ASMM) Project of NASA's Aviation Safety program is cultivating sources of data and developing automated computer hardware and software to facilitate efficient, comprehensive, and accurate analyses of the data collected from large, heterogeneous databases throughout the national aviation system. The ASMM addresses the need to provide means for increasing safety by enabling the identification and correct-

ing of predisposing conditions that could lead to accidents or to incidents that pose aviation risks.

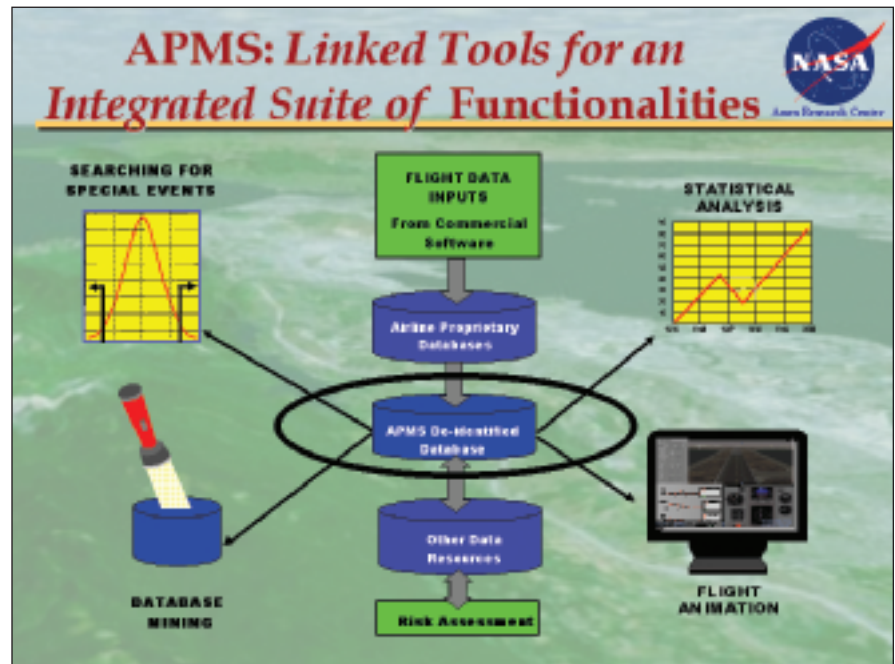
A major component of the ASMM Project is the Aviation Performance Measuring System (APMS), which is developing the next generation of software tools for analyzing and interpreting flight data (see figure). Airlines, military units, corporate operators, and others analyze aircraft flight data to identify contributing factors and

corrective actions for situations in which aircraft performance parameters exceed normal limits during phases of flight. The programs for performing such exceedence-based analyses are denoted flight operations quality assurance (FOQA in civilian settings) programs and take their inspiration from statistical process control. However, FOQA analysis involves use of only a portion of the data: large quantities of data are scanned to extract and under-

stand a small number of predefined events. The sets of data contain far more information that is potentially helpful for understanding and enhancing the safety, reliability, and economy of flight operations.

The challenge is to find and understand key information from the mass of data generated by aircraft and collected by data recorders. There is a need to automate scanning, analysis, and reporting to produce meaningful information upon which human analysts can act. The APMS software is intended to satisfy this need. Beginning with workload enhancements to exceedance-based FOQA analyses and progressing to sophisticated multivariate statistical analyses, the APMS has developed key software tools to advance the science of flight-data analysis.

Another major component of the ASMM Project is the Performance Data Analysis and Reporting System (PDARS), which is developing networking and analysis hardware and software for application air-traffic-control (ATC) radar data. PDARS, which was developed jointly with the Federal Aviation Administration (FAA) Office of System Capacity, provides ATC decision-makers at the facility level with a comprehensive means of monitoring the health, performance, and safety of day-to-day ATC operations. PDARS enables analysis of daily operation of the National Airspace System (NAS) at local and inter-facility levels. By translating flight-track and flight-plan data into useful performance information, PDARS significantly augments the abil-



The **Aviation Performance Measuring System** — a component of NASA's Aviation Safety Monitoring and Modeling (ASMM) Project — is developing the means of automated processing of large collections of flight data to help answer questions pertaining to performance and safety.

ity of the FAA to adjust operational procedures and techniques. The net outcomes of these adjustments are quantifiable improvements in safety and efficiency throughout the NAS.

Future progress in aviation safety can be expected to involve the routine integration of information from APMS, PDARS, and other sources. Such integration will require both greater depth of analysis of individual data sources and automated ability to integrate information extracted from diverse sources to draw sound conclusions on

causal factors and risk assessment. It also will be necessary for users to evaluate such integration to determine its usefulness. It is planned to develop capabilities for such integration during the next few years.

This work was done by Thomas R. Chidester and Irving C. Staller of Ames Research Center. Further information is contained in a TSP (see page 1).

Inquiries concerning rights for the commercial use of this invention should be addressed to the Patent Counsel, Ames Research Center, (650) 604-5104. Refer to ARC-14362-1.



Multimode-Guided-Wave Ultrasonic Scanning of Materials

Two documents discuss a method of characterizing advanced composite materials by use of multimode-guided ultrasonic waves. The method at an earlier stage of development was described in "High-Performance Scanning Acousto-Ultrasonic System" (LEW-17601-1), *NASA Tech Briefs*, Vol. 30, No. 3 (March 2006), page 62. To recapitulate: A transmitting transducer excites modulated (e.g., pulsed) ultrasonic waves at one location on a surface of a plate specimen. The waves interact with microstructure and flaws as they propagate through the specimen to a receiving transducer at a different location. The received signal is analyzed to determine the total (multimode) ultrasonic response of the specimen and utilize this response to evaluate microstructure and flaws. The analysis is performed by software that extracts parameters of signals in the time and frequency domains. Scanning is effected by using computer-controlled motorized translation stages to position the transducers at specified pairs of locations and repeating the measurement, data-acquisition, and data-analysis processes at the successive locations. The instant documents reiterate the prior description and summarize capabilities of the hardware and software of the method at the present state of development. One document presents results of a scan of a specimen containing a delamination.

This work was done by Don Roth of Glenn Research Center. Further information is contained in a TSP (see page 1).

Inquiries concerning rights for the commercial use of this invention should be addressed to NASA Glenn Research Center, Commercial Technology Office, Attn: Steve Fedor, Mail Stop 4-8, 21000 Brookpark Road, Cleveland, Ohio 44135. Refer to LEW-17527.

Algorithms for Maneuvering Spacecraft Around Small Bodies

A document describes mathematical derivations and applications of autonomous guidance algorithms for maneuvering spacecraft in the vicinities of small astronomical bodies like comets or asteroids. These algorithms compute

fuel- or energy-optimal trajectories for typical maneuvers by solving the associated optimal-control problems with relevant control and state constraints. In the derivations, these problems are converted from their original continuous (infinite-dimensional) forms to finite-dimensional forms through (1) discretization of the time axis and (2) spectral discretization of control inputs via a finite number of Chebyshev basis functions. In these doubly discretized problems, the Chebyshev coefficients are the variables. These problems are, variously, either convex programming problems or programming problems that can be convexified. The resulting discrete problems are convex parameter-optimization problems; this is desirable because one can take advantage of very efficient and robust algorithms that have been developed previously and are well established for solving such problems. These algorithms are fast, do not require initial guesses, and always converge to global optima. Following the derivations, the algorithms are demonstrated by applying them to numerical examples of fly-by, descent-to-hover, and ascent-from-hover maneuvers.

This work was done by A. Bechet Acikmese and David Bayard of Caltech for NASA's Jet Propulsion Laboratory. Further information is contained in a TSP (see page 1).

The software used in this innovation is available for commercial licensing. Please contact Karina Edmonds of the California Institute of Technology at (626) 395-2322. Refer to NPO-41322.

Improved Solar-Radiation-Pressure Models for GPS Satellites

A report describes a series of computational models conceived as an improvement over prior models for determining effects of solar-radiation pressure on orbits of Global Positioning System (GPS) satellites. These models are based on fitting coefficients of Fourier functions of Sun-spacecraft-Earth angles to observed spacecraft orbital motions. Construction of a model in this series involves the following steps:

1. Form 10-day "truth" orbit arcs from precise daily GPS orbit data gathered during more than four years.
2. Construct a model of the solar-radia-

tion pressure and estimate model-parameter values that make a least-squares best fit of the model-predicted trajectory to each of the "truth" 10-day orbit arcs.

3. Using a least-squares procedure and utilizing the full covariance information from each 10-day fit, combine the estimates from all satellite arcs into a single set of model parameters for the two GPS constellations of the satellites now or soon to be placed in service.
4. Evaluate the model thus derived by means of orbit-data-fit and orbit-prediction tests.

In evaluations performed thus far, these models have been found to offer accuracies significantly greater than those of the prior models.

This work was done by Yoaz Bar-Sever and Da Kuang of Caltech for NASA's Jet Propulsion Laboratory. Further information is contained in a TSP (see page 1). NPO-41395

Measuring Attitude of a Large, Flexible, Orbiting Structure

A document summarizes a proposed metrology subsystem for precisely measuring the attitude of a large and flexible structure in space. Two cameras would be mounted at the base of the structure:

- (1) A star camera equipped with two separate fields of view: (a) imaging stars in the background near the structure tip while excluding the tip from view to prevent saturation from sunlight reflected from the tip, and (b) imaging the tip and have simultaneous stars in the background. First, in the absence of reflected sunlight and with the self-illuminated fiducials on the structure turned off, the star camera would open both fields of view and establish the angular relationship between the two fields of view.
- (2) The second camera (metrology camera) is too insensitive to observe stars but sensitive enough to image a number of bright self-illuminated fiducials on the structure through a narrow band pass filter (even in the presence of sunlight) at high rates. Still in the absence of sunlight, the self-illuminated fiducials at the tip of the structure are imaged simultane-

ously by the star and metrology cameras to establish the relationship between the two different cameras.

During operations, the star camera would be operated in the tip-excluding configuration while the metrology camera tracked the tip. The orientation of the base to tip line relative to the stars would be determined by use of informa-

tion from the metrology camera, the star camera, inertial measurement unit (IMU), and calibration data. The advantage of the proposed scheme is (1) it is possible to obtain attitude knowledge at high rates (based on IMU and metrology camera); (2) it is possible to operate when the antenna is illuminated by the Sun; and (3) it is possible to perform on-

orbit alignment after launch.

This work was done by Carl Christian Liebe, Randall Bartman, Alexander Abramovici, Jacob Chapsky, Edward Litty, and Keith Coste of Caltech for NASA's Jet Propulsion Laboratory. Further information is contained in a TSP (see page 1). NPO-41411



National Aeronautics and
Space Administration